PLANETARY RADIO EMISSIONS FROM LOW MAGNETIC LATITUDES: OBSERVATIONS AND THEORIES

Dyfrig Jones

Space Plasma Physics Group,
British Antarctic Survey, NERC,
Madingley Road, Cambridge, CB3 OET, UK

Abstract

Recent observations of planetary radiations from low magnetic latitudes are reviewed. At Earth a major source of nonthermal continuum is Terrestrial Myriametric Radiation (TMR) from the equatorial plasmapause and from the magnetopause. The theories proposed for the production of TMR are listed and their predictions are compared with satellite observations. The application of the theories to Jovian Kilometric Radiation (KOM), the radio emission at Jupiter which has been suggested to be the analogue of TMR, is reviewed. The implications of the TMR and KOM results for radiations observed at Saturn and Uranus are briefly considered.

1. Introduction

Within the context of this review, radio emissions are defined as being those which are capable of escaping from the magnetospheres wherein they are created (see Jones, 1982b). They are radiations propagating in the ordinary (O) and extraordinary (X) electromagnetic "free–space" modes. Other modes, such as electron–cyclotron and ion–cyclotron waves, which are not free to escape and to be observed outside the magnetospheres are not discussed. Exceptions will be made, however, for those electrostatic and electromagnetic emissions, such as upper–hybrid and Z–mode waves, which cannot themselves propagate very far from their sources but which are believed to be involved in the generation of radio emission which can ultimately escape.

Another constraint imposed on this review is that it will not address auroral radio emissions – terrestrial and Saturnian kilometric, and Jovian decametric radiations – whose source mechanism (Wu and Lee, 1979; Wu et al., 1982) are generally believed to differ from those to be discussed here and which are reviewed elsewhere (Wu; Le Quéau, this volume). Therefore the emissions which will be considered are terrestrial and Saturnian myriametric and Jovian kilometric radiations; also nonthermal continuum radiation which seems to derive predominantly from the foregoing emissions, at least for the Earth, will be briefly touched upon. The review will deal in turn with Earth, Jupiter, Saturn and Uranus. It is not the intention to dwell on the observations, theories and results obtained pre–1984 which have been covered comprehensively in previous reviews (Jones, 1985; Kurth, 1986), but to discuss the relevant information obtained during the past three to four years.

2. Earth

There is overwhelming evidence that the predominant source of terrestrial myriametric radiation (TMR) is electrostatic upper–hybrid (ESUH) waves which are most intense at the magnetic equator at and beyond the plasmapause (see Jones, 1985 and references therein). By means of some process, for which there have been numerous theories proposed, the ESUH wave energy is converted to electromagnetic TMR which propagates away through the magnetospheric cavity. The same mechanism is believed to be operating at the magnetopause which has more recently been identified as a second source of TMR (Jones, 1985, 1987a; Budden and Jones, 1986). TMR at frequencies less than the magnetosheath plasma frequency is trapped within the magnetospheric cavity and, after multiple reflection and mixing of radiation from numerous sources, forms nonthermal continuum radiation. The continuum is observed to contain both ordinary (O) and extraordinary (X) modes, and it has been a moot point whether this mixture appears in the parent TMR or only in the continuum due to the subsequent multiple reflection process. TMR at frequencies greater than the magnetosheath plasma frequency escapes from the magnetosphere and propagates away through the interplanetary medium (Gurnett, 1975).

On the theoretical front there has been no new theory proposed since the review by Jones (1985) except for that of Rönnmark (1985). Hence the total number of theories suggested to date stands at seven, three of which are linear, the remainder being non–linear. The linear theories are those of Frankel (1973) who suggested that continuum was created directly by gyrosynchrotron emission, that of Jones (1976a,b; 1980), who invoked linear mode conversion of electrostatic upper–hybrid and electromagnetic Z–mode waves to O–mode radiation via radio windows, and that of Okuda et al. (1982) and Ashour–Abdalla and Okuda (1984) who proposed what appears to be resonance tunnelling (Budden 1961; 1985) of energy from the upper–hybrid mode to the free space modes. There has been no further work done on these theories except for that of Jones which will be considered later.

There has similarly been no further work of which the author is aware on the non–linear theories of Melrose (1981), Rönnmark (1983), and Christiansen et al. (1984) all of whom proposed wave–wave interaction or coalescence of ESUH waves with some low frequency waves or density irregularities. However, Rönnmark (1985) has suggested a variation of the above in which the TMR would appear as a result of the parametric decay of intense ESUH waves, the other decay product being low frequency waves. A major problem with all these non–linear theories is the absence, in the apparent source regions, of the low frequency waves required by, or resulting from, the conversion mechanisms proposed. Until such evidence appears and until further work is done on these theories the reader is referred to the previous reviews and to the original papers.

A number of aspects of the linear mode conversion "window" (LMCW) theory, however, have been subjected to recent study. The LMCW theory has been described in detail elsewhere, Jones (1976a,b; 1980; 1981a,b,c; 1982a; 1983a,b; 1984a,b; 1985; 1986a,b; 1987a,b) and only a brief summary is presented here. The theory requires that the plasma density gradient ∇N in the source region be nearly perpendicular to the magnetic field vector

B_o. This allows the ESUH waves to propagate without damping with their wave vectors nearly normal to B_o, such that they become electromagnetic Z–mode waves which lie on the same dispersion branch (Ginzburg, 1970; Oya, 1971). These Z–mode waves, in turn, propagate in the density gradient and, when their frequency equals the local plasma frequency f_p, they can gain access to a radio window whereby they convert to 0–mode radiation. This is TMR, which propagates to lower densities and, provided that there are no large irregularities in its path, its direction of propagation is predominantly controlled by the initial conditions at the radio window. This property has been used for remote–sensing of the source regions. The various steps in the LMCW theory can be more clearly understood by reference to Figure 1.

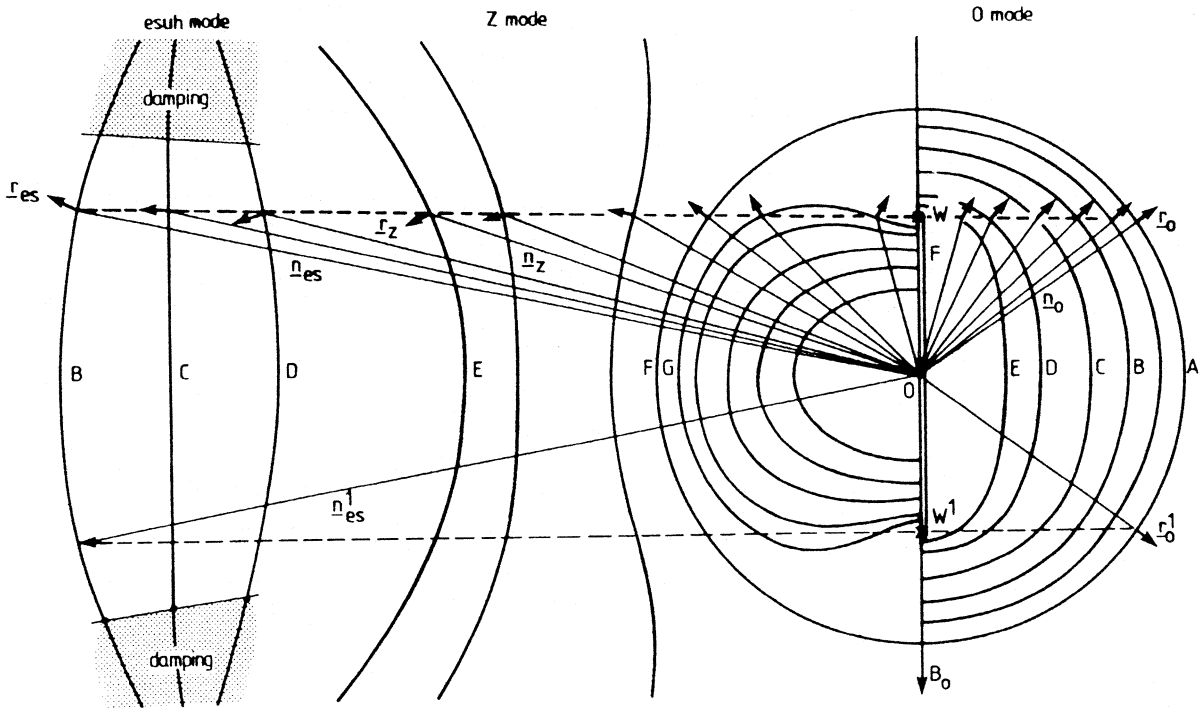

Fig. 1a: Sketch (from Jones and Leblanc, 1987) of refractive index contours of ESUH, Z, and O–mode waves, at frequency f. The contours are for different values of the plasma frequency, f_p, with f_p increasing towards the origin (i.e. from A, B, ..., to O). The density gradient is normal to the magnetic field B_o. The symbols n and r represent wave–normal and ray directions respectively.

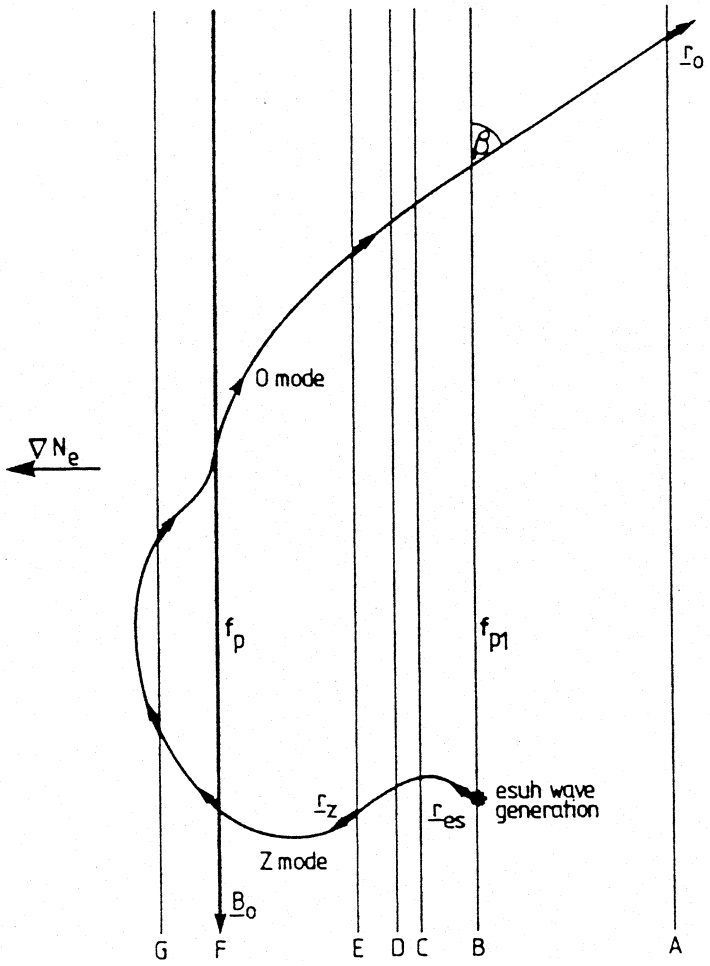

Fig. 1b: Ray path corresponding to Figure 1a. The density gradient ∇N_e is normal to the magnetic field B_o. The isoionic contours A – G correspond to the refractive index contours A – G in Figure 1a.

Consider ESUH waves of frequency f to be produced by energetic electrons at the level where the plasma frequency is f_{p1}. The refractive index surface of these waves is labelled B on the left in Figure 1a. If one singles out initially one wave, for example that having wave–normal $\underline{n}_{es}$, then it is a well–known property of refractive index surfaces in a loss–free plasma (see Budden, 1985, for example) that the direction of energy travel – the ray direction $\underline{r}_{es}$ – is normal to the refractive index surface at the tip of $\underline{n}_{es}$. As the wave travels in direction $\underline{r}_{es}$ into a higher plasma density it encounters an increased f_p and its refractive index surface could then probably be represented by contour C on the left in Figure 1a. As the density gradient is normal to B_o, Snell's law of refraction requires that the component of the wave–normal parallel (or antiparallel) to B_o remains constant as the wave propagates. Therefore the tip of the wave–vector which now lies on surface C must, as the wave propagates, also lie on the dashed line drawn perpendicular to B_o through the tip of $\underline{n}_{es}$. Further propagation into higher densities takes the wave–normal on the surface D, its tip remaining on the dashed line. At each step the ray direction is given by the normal to the surface at the tip of the wave–normal. Provided that the wave–normals in the electrostatic wave region are nearly perpendicular to B_o the waves will propagate undamped. Hence it is a requirement in the linear conversion theory that ∇N_e be nearly normal to B_o to avoid rotation of the wave–normals into the damping regions marked in

Figure 1a. In this context it should be borne in mind that the refractive index surfaces of the ESUH waves sketched in the figure have not been drawn to scale: in reality the ESUH surfaces should lie at a distance from the origin 0 a few hundred times the distance of contour F from the origin and their general form can be seen in Lembege and Jones (1982). As the waves propagate they gradually become more electromagnetic. On encountering refractive index surface E, for example, they may well have converted naturally into electromagnetic Z–mode waves, and will continue as such until they reach the window level at W, where the plasma frequency equals the wave frequency. At this point the waves can be converted into 0–mode radiation, the conversion being 100% efficient if the plasma is cold and collisionless and if the dashed line passes through the window point W as it does in the figure. The 0–mode radiation, which must also satisfy Snell's law, propagates away into lower densities with its wave–normal rotating until it becomes close to its free space position $\underline{n}_o$, in Figure 1a, which lies in the plane containing B_o and the density gradient. To envisage how the wave could actually propagate in the plasma one is referred to the sketch in Figure 1b which is a rough representation of the ray path in real space.

In Figure 1b the isoionic contours corresponding to the refractive index surfaces in Figure 1a are similarly labelled A–F; because ∇N_e is normal to B_o the isoionic contours are assumed to be aligned parallel to the magnetic field B_o. Waves of frequency f in the ESUH mode are generated at level B where the plasma frequency is f_{p1}. The wave propagates initially in direction $\underline{r}_{es}$, passes levels C and D and reaches level E where it becomes a Z–mode wave propagating in direction $\underline{r}_z$. Further propagation takes it past levels F and G beyond which it undergoes a reflection. On again reaching level F it converts into an O–mode wave at the window and then propagates away to lower densities, ultimately travelling in the direction $\underline{r}_o$ in free space, at level A, $\underline{r}_o$ also lying in the plane containing B_o and the density gradient. It is seen that the direction r_o makes an angle β with respect to the source magnetic field line and it can be easily deduced from Figure 1a that β depends on distance of W from the origin O. It can be shown that this distance depends on the ratio of the plasma frequency to the cyclotron frequency at the window level F (Jones, 1980); in fact $\beta = \arctan (f_p/f_c)^{1/2}$. For the density gradients encountered in TMR source regions at the plasmapause and in the proposed KOM sources at the Io torus it can be shown that the distance between levels F and B is small so that the refraction of the 0–mode wave occurs in the close vicinity of the window level, and thereafter the ray path in the magnetospheric cavities can usually be assumed to be linear.

From Figure 1a it is seen that the refractive index surfaces are symmetrical about a horizontal line through origin 0, and that there exists another window W^1 for ESUH waves which start with wave normal $\underline{n}^1_{es}$. It is clear that the ray path corresponding to propagation through this second window will be symmetrical to that shown in Figure 1b, the final 0–mode ray direction pointing along $\underline{r}^1_o$ at angle β to the magnetic field. In this simplified picture, therefore, a source of ESUH waves with initial wave normals $\underline{n}_{es}$ and $\underline{n}^1_{es}$ will result in two beams of 0–mode radiation. If the source is located at the magnetic equatorial plane, one beam will be in the northern hemisphere, the other in the southern hemisphere, the angle between them being $(\pi - 2\beta)$.

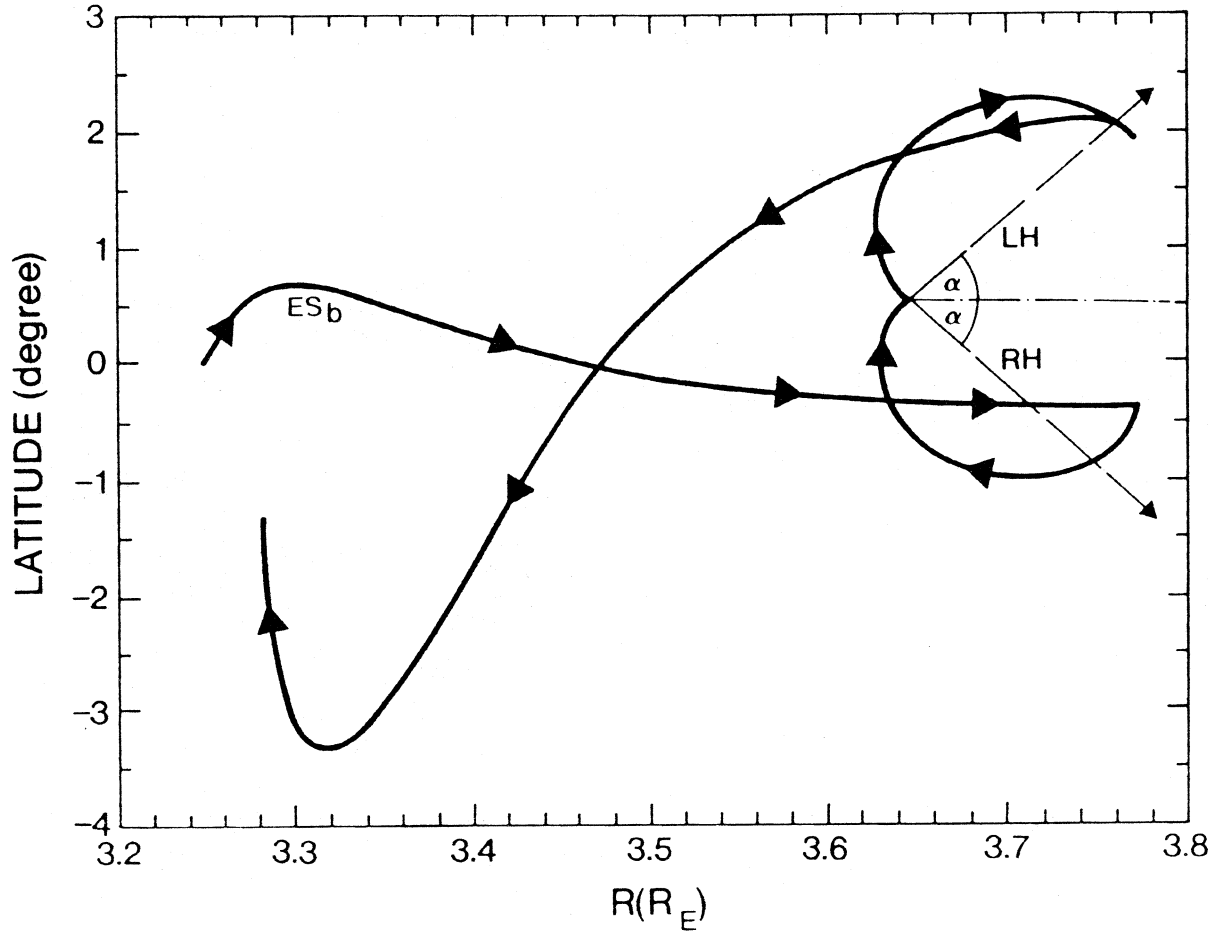

Fig. 2: Sketch of ray path of ESUH, Z, and O–mode 28.015 kHz wave. The ESUH wave is started at the equator at 3.25 R_E where $f = 1.1\ f_c$, with wave–normal in the magnetic meridian plane and at angle 89.74° relative to the magnetic field line. The wave first propagates as a backward–propagating electrostatic wave (ES_b), is reflected at $\sim$ 3.78 R_E, where $f \simeq f_{uh}$, into a forward–propagating Z–mode wave which, in turn, is reflected at $\sim 3.63R_E$ and, at the radio window at $\sim 3.65R_E$, where $f \simeq f_p$, can be converted into a freely propagating O–mode wave whose polarization is left–handed (LH) and which makes angle α with the normal to the magnetic field line, the normal being approximately the magnetic equator in this instance. The Z–mode energy which is not converted at the window reflects and follows a nearly symmetrical propagation path and is ultimately absorbed in the plasma at $\sim 3.3.R_E$. Reversing the wave–normal at this point results in the wave retracing the path shown with again conversion at the window level (through the other window) into right–hand (RH) polarized O–mode radiation. (Polarization here is that which would be determined by a spacecraft in the magnetospheric cavity). The angle between the two O–mode beams is 2α. (This figure is based on Yamaashi et al. (1987), Figure 16c).

In reality ESUH waves at the level B, where the plasma frequency is f_{p1}, are expected to be produced with a range of wave–normal angles between the limits of damping on contour B in Figure 1a. It can be shown that those which do not satisfy the condition for propagation through the windows are reflected and ultimately absorbed in the plasma (Jones, 1980; Lembege and Jones, 1982; Hashimoto et al., 1987; Horne, 1988).

Ray paths in a realistic plasmapause gradient were computed by Lembege and Jones (1982) using Poeverlein's construction for the electrostatic wave portions of the ray path and with a ray–tracing computer program for the electromagnetic portion. These ray paths have since been confirmed and others computed using a ray–tracing computer program for the whole path by Yamaashi et al. (1987), Hashimoto et al. (1987) and Horne (1987; 1988), and Figure 2 shows an example based on a figure from the first paper cited.

In Figure 2, the electrostatic wave of frequency $f = 1.1\ f_c$ is started at the equator at $3.25R_E$ with its wave–normal angle at 89.74° relative to the dipole magnetic field and lying in the meridian plane on the earthward side of the field line. As the wave is initially a backward–propagating electrostatic wave (see Lembege and Jones, 1982, for example), the ray travels to larger radial distances (decreasing f_p and f_{uh}) while the wave–vector has a large inward component. At $\sim 3.78R_E$ where $f \simeq f_{uh}$ the wave becomes a forward–propagating Z–mode wave, which moves back inwards towards the Earth. It crosses the level at $\sim 3.65R_E$ where $f \simeq f_p$ and is reflected at $\sim 3.63R_E$; it then experiences a spitze reflection (Budden 1961, 1985) on again reaching the level $f \simeq f_p$. It is at this point that the wave can encounter the radio window and be converted into an 0–mode wave which propagates away from the Earth through the magnetospheric cavity. The energy which is not converted at this level, reflects and travels first in and then out in the Z–mode to become electrostatic again where $f = f_{uh}$ and it ultimately returns its energy to the particles, being absorbed on arriving back near the source region $< 3.3R_E$ at latitude $\simeq -1.3°$.

In reality, the windows W and W^1 in Figure 1a are not infinitesimal points but areas in refractive index space, whose dimensions depend on the magnitude of the density gradient $|\nabla N|$, on the wave frequency f and on its ratio f/f_c to the cyclotron frequency. Full–wave computations of transmission and reflection of waves at TMR radio windows using realistic plasma parameters have been presented by Budden and Jones (1986; 1987a,b) and Jones (1987a). To understand those results, the most important of which will be shown here, it is necessary to define the coordinate system in which they are presented.

Figure 3 shows a sketch of the two beams of radiations which emerge through the window apertures W and W^1. The figure is, in fact, a portrayal of refractive index space overlaid on real space. The magnetic field and density gradient vectors B_o and ∇N, which are perpendicular, are in both spaces whereas the two beams are in real space, but the window apertures, the unit sphere and the angles β, ϕ and ψ are in refractive index space.

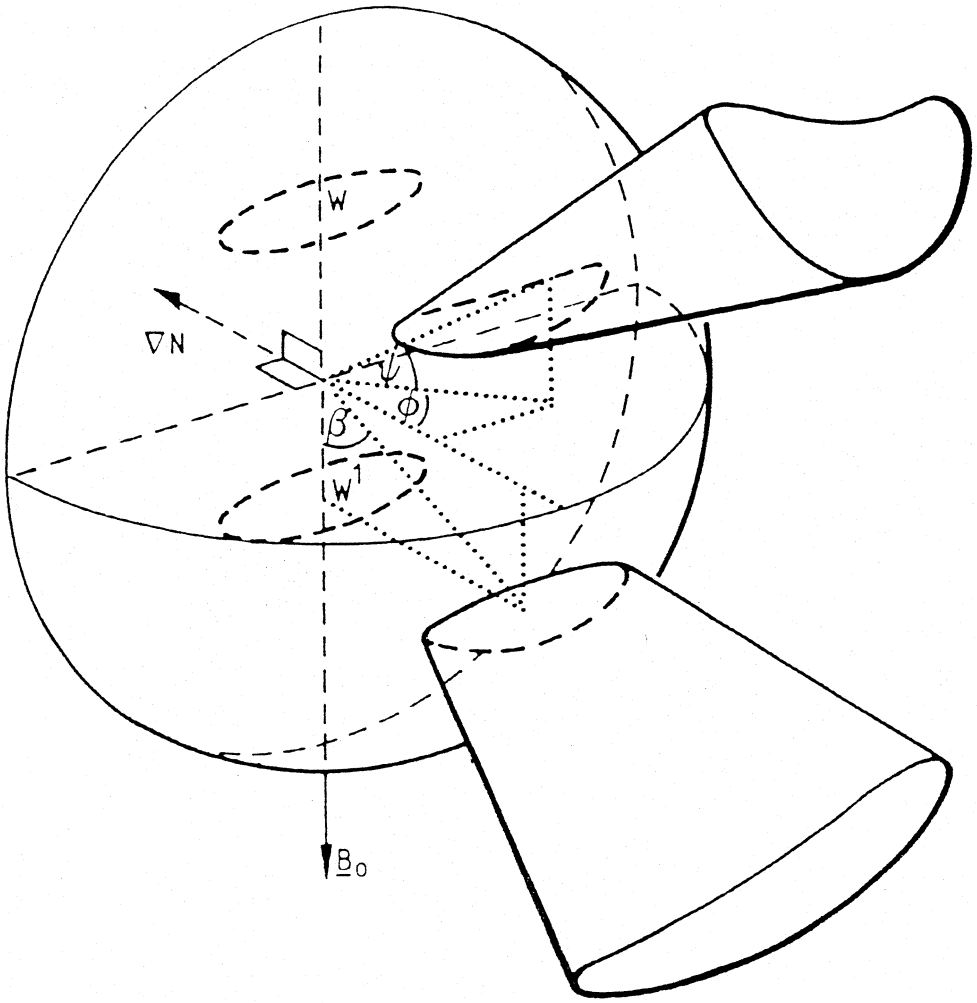

Fig. 3: Sketch of beaming of radiation which has propagated through the radio windows W and W^1. The angle between the centres of the beams and the magnetic field line is β. Angles ϕ and ψ define other positions in the beams. (Thus the beam centres are $\phi = 0$, $\psi = \pm(\pi/2 - \beta) = \pm\alpha$.)

Figure 4 shows the extent, in the $\phi - \psi$ domain, of a radio window at the plasmapause; it can be visualized as the beam cross–section at the unit sphere in Figure 3. The magnitudes of f, f_c, ∇N were estimated from a TMR event studied by Kurth (1982), and the electron temperature was assumed to be 11.6 x 10^3K corresponding to an electron thermal energy of 1eV, typical of the plasmapause. It can be seen in Figure 4 the large extent of the radio window, with the 6 dB half widths in ϕ and ψ for the 0–mode being about 40° and 5° respectively. The X–mode radiation intensity was found to be negligible in comparison, being at least 26 dB less than that of the 0–mode; it has therefore been omitted from Figure 4. At the centre of the 0–mode window, where $\phi = 0°, \psi = arctan(f_c/f_p)^{1/2} \simeq$ 17.5°, there is virtually complete conversion (0 dB emergent 0–mode level) from the incident plasma/Z–mode wave to the 0–mode. The attenuation of the plasma, which is reflected during conversion, appears in the upper frame of Figure 4.

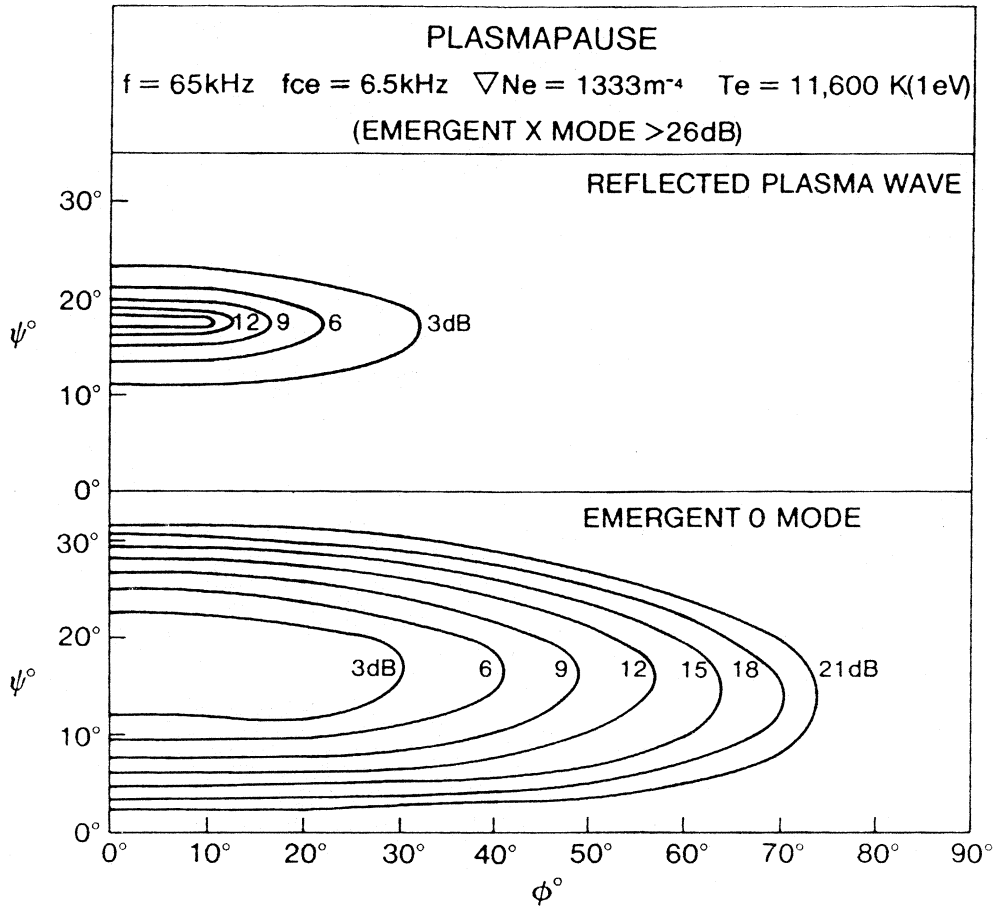

Fig. 4: Full–wave, warm plasma computations of mode conversion at the plasmapause (from Budden and Jones, 1987a). Lower frame shows contours of constant converted energy (emergent O–mode) in dB. Upper frame shows similar contours of reflected, unconverted energy. The axes are labelled ϕ, ψ which refer to the angles shown in Figure 3. Emergent X–mode energy is negligible compared with that of the O–mode and is not shown.

Similar computations for a magnetopause source are shown in Figure 5 (from Jones, 1987a). The plasma parameters used are those obtained from a TMR event presented by Etcheto et al. (1982) the radiation being identified by Jones (1985) as being from a magnetopause source; the electron thermal energy was assumed to be 200 eV (Eastman and Hones, 1979). The large 0–mode window is again clearly evident but also apparent is the emergent X–mode radiation whose total power over the $\phi - \psi$ plane may well rival that of the 0–mode.

The above full–wave results led to the conclusion that the 0–mode TMR window apertures are much larger than had earlier been anticipated; also that the plasmapause and magnetopause are sources of 0–mode TMR whereas a significant amount of X–mode TMR is probably expected only from the magnetopause. Thus it seems that the 0 and X components observed in nonthermal continuum have their sources in the parent TMR, although the distribution of energy in the two modes may also be affected by the multiple reflection process at the walls of the magnetospheric cavity (Jones, 1976b; 1980; Barbosa, 1981).

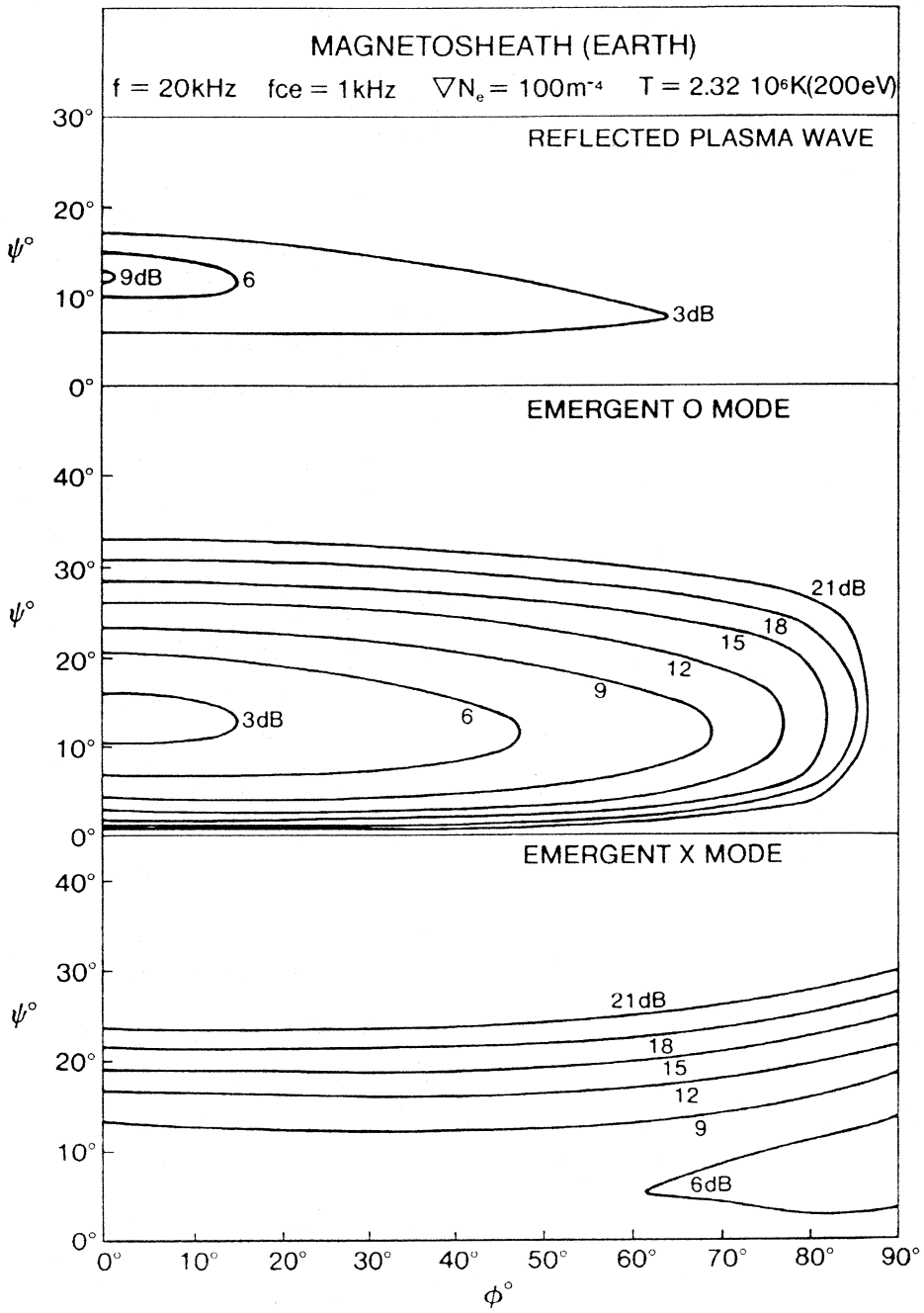

Fig. 5: Full wave, warm plasma computations of the conversion at the magnetopause of ESUH/Z–mode waves to O and X–mode waves (lower two frames) and of the amount of reflected, unconverted energy (top frame). Angles ϕ, ψ are as defined in Figure 3. Note that significant conversion occurs for both O and X–modes.

Fig. 6 (color plot): A spectrogram obtained from the plasma wave instrument (PWI) on the Dynamics Explorer 1 satellite during a south to north pass through the magnetic equator. (Based on Jones et al. (1987), Figure 1). Wave intensity is color–coded with increasing intensity going from black, through blue, to red and white. Note the two blocks of TMR, which lie on either side of the magnetic equator, and which have features which repeat themselves from one block to another as the satellite moved consecutively through the beams from south to north.

Reference to Figures 1 to 4 will show that, if the source ESUH waves are fairly tightly confined to the magnetic equatorial plane as is often observed to be the case (Gough et al., 1979), the TMR from the plasmapause sources should lie in two beams, one to the northern and the other to the southern hemisphere. Evidence had been presented earlier (Jones, 1980), using GEOS 1 data, for the existence of the northern beam but the lack of a suitably equipped satellite in an appropriate orbit proved a stumbling block to the near–instantaneous observation of the two beams. Recently, however, results from the Plasma Wave Instrument (PWI) on the satellite Dynamics Explorer 1 (DE–1) conclusively showed for the first time the existence of both TMR beams (Jones et al., 1987).

Figure 6 is a frequency–time spectrogram which shows wave electric–field intensities from the Plasma Wave Instrument, PWI, on DE–1. During the interval shown, the PWI was connected to a 200–m electric dipole antenna located in the spin plane of the spacecraft. The ordinate shows the frequency scale (logarithmic) and the abscissa shows the Universal Time (UT), the magnetic latitude (λ_m) and the radial distance (R_E) of DE–1. The local electron cyclotron frequency (f_c) and its harmonics ($2f_c - 4f_c$) are plotted directly on the spectrogram as white dotted lines. At frequencies above f_c, and in a very limited latitude range near the magnetic equatorial plane, emissions are seen between the lower harmonics of f_c. These are identified as $(n + 1/2)f_c$ electrostatic electron–cyclotron harmonic emissions (see Ashour–Abdalla and Kennel, 1978, for example). The most intense member of this family lies at a higher frequency, $f \simeq 62.5$ kHz, which is believed to be the upper hybrid resonance frequency $f_{UHR} = (f_c^2 + f_p^2)^{1/2}$, where $f_p = 9N_e^{1/2}$ Hz is the electron plasma frequency and N_e is the electron concentration in m^{-3}. When DE–1 crossed the equatorial plane, f_c was 7.6 kHz which is much less than f_{UHR}; thus $f_{UHR} \simeq f_p$. This condition would appear to be true for most of the portion of the orbit shown. Hence the relatively weak band of noise, just at the limit of visibility in Figure 6 in the range 60–100 kHz after 10:30 UT, is identified as nonthermal continuum radiation whose lower frequency limit is believed to lie near to the value of f_p along the satellite trajectory (Gurnett, 1975).

The radiation of main interest here is seen as two distinct "blocks" near 100 kHz embedded in the nonthermal continuum on either side of the intense upper hybrid emission recorded at the equatorial crossing, and at a slightly higher frequency. The two blocks are seen to be nearly identical and are separated by a zone of virtually no emission (except continuum) near the equatorial plane. They are symmetric, but not mirror images, about the equatorial plane and, as will be shown shortly, are propagating in the directions predicted by the LMCW theory. It should also be noted that there is a single block of emission straddling the upper hybrid event right at the magnetic equator which may also be TMR, the satellite in this case possibly being so close to the source that the two beams overlap.

The equation $\beta = \pm \arctan(f_p/f_c)^{1/2}$, for the beam angle relative to the magnetic field line B_o at the window, can be used for remote–sensing the source location (Jones, 1983a). Given that TMR of frequency f is emitted where $f = f_p$ and that it is beamed with respect to the source magnetic field at the above angle β, which depends on f_p and f_c, one may determine, for a given magnetic field model, where an observer has to be located in order

to receive the radiation. Conversely, knowing the magnetic coordinates of the observer, one can compute the possible positions of the sources in a magnetic field model. For the Earth, it may be assumed that the magnetic field is dipolar within about $4R_E$. If one concentrates on possible sources in the vicinity of the equatorial plane, the location and dimension of the TMR source in Figure 6 can be determined and is shown in Figure 7 (see Jones et al., 1987 for details). The TMR is found to emanate from a steep density gradient just within 4.0 R_E and to extend in magnetic latitude $\lambda_m \simeq \pm 0.4°$. This source position was confirmed by independent direction–finding by the PWI using the satellite's spin, the measured directions γ and δ being also shown in Figure 7. These results would appear to provide the strongest evidence to date for the validity of the LMCW theory. Unfortunately the TMR emissions in Figure 6 were too weak for reliable polarization analysis and another, stronger event under study shows that the polarization of the two beams is as predicted by the LMCW theory (Gurnett et al., 1988).

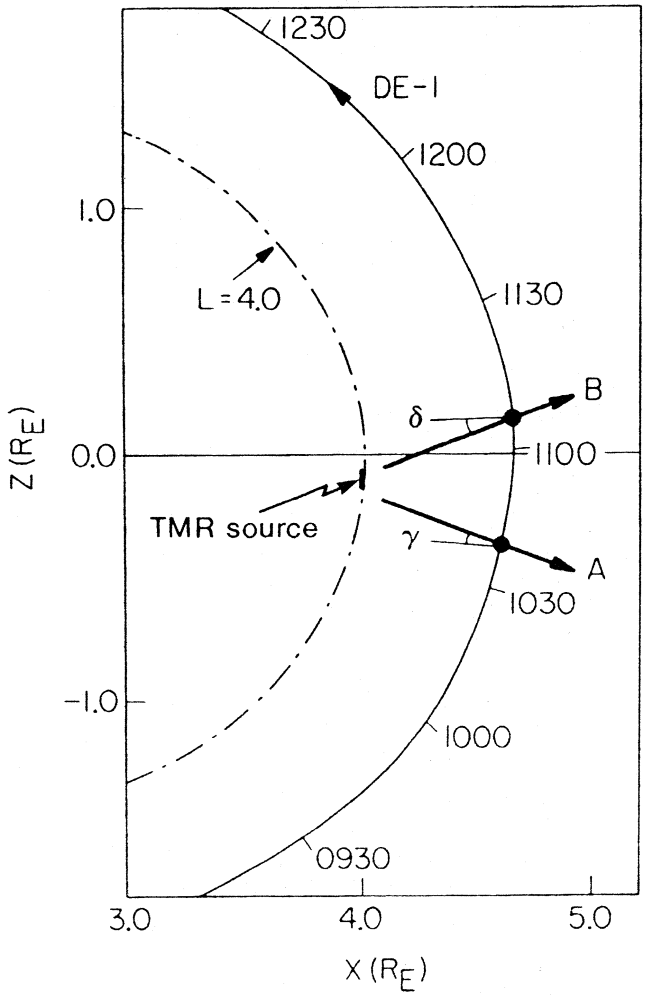

Fig. 7: The propagation directions (arrows A and B), for the two TMR blocks shown in Figure 6, as determined from the intensity modulation of the signals received by the PWI as DE–1 was cartwheeling along its orbit. The location of the TMR source as determined by remote–sensing is also indicated (see Jones et al., 1987 for details), and is in excellent agreement with the source inferred from directions A and B. (Note that the equator, as drawn, corresponds to a model magnetic field; as determined from the UHR emission in Figure 6, the actual equator, is straddled by the source region shown).

The polarization of radio emissions has been a parameter of great importance in the study of radio sources and source mechanisms. However, it has often been difficult to determine how an observed polarization, perhaps at considerable distance from the wave's point of origin, is related to the polarization at the source. The reason for this difficulty is obvious – a radio wave's polarization in a plasma depends on the magnetic field. For this reason Budden and Jones (1987c) have studied theoretically the polarization of waves in magnetospheric cavities where the plasma density is relatively low and the magnetic field is that of a dipole and thus changes in magnitude and orientation along the propagation path. It was shown that the polarization of TMR produced initially in the 0 (or X)–mode remains close to that of a locally produced 0 (or X) wave with the same wave–normal direction, provided that the plasma frequency (i.e. the plasma density) exceeds a minimum value which depends on the direction of the propagation path.

The success of the LMCW theory in describing and predicting the observed properties of TMR seems to have been paralleled by similar success in explaining the source locations and characteristics of analogous radiations at the other planets as will be shown in the following sections.

3. Jupiter

The study of Jovian nonthermal continuum, and Jovian broadband and narrowband kilometric radiations, bKOM and nKOM, has continued apace during the past three years.

3.1 Jovian continuum radiation

An investigation of Jovian 1.2 kHz continuum radiation recorded by the Planetary Radio Astronomy (PRA) experiment (Warwick et al., 1977) on Voyagers has been conducted by Leblanc et al. (1986) and Rucker et al. (this volume). The continuum was observed in the magnetospheric cavity on both the dayside and nightside, being most intense in the magnetotail lobes when Voyagers were above and below the plasmasheet. The observations were considered within the context of other plasma waves recorded within the Jovian magnetosphere and, by a process of elimination, it was suggested that the most likely source of the 1.2 kHz Jovian continuum is the morning/ prenoon magnetopause. Further evidence for a magnetopause source for Jovian continuum recorded by the Plasma Wave System experiment on Voyagers comes from a study of frequencies near 3 kHz by Kurth et al. (1986b). This study of periodic variations in the amplitude of continuum shows structure with periods near 5 and 10 hours. It was stated that this structure is not organised by the position of the observer relative to the plasma sheet but rather it appears because of preferred orientations of System III Longitude with respect to direction to the sun. This implies a clocklike modulation of continuum radiation intensity which, it is stated, has the implication that the source region is near the magnetopause and may somehow indirectly connect with the generation to the clocklike modulation of energetic (MeV) electron fluxes from the dawn magnetopause of Jupiter (Schardt et al., 1981).

It should be added that Barbosa (1987) questioned Kurth et al.'s (1986b) interpretation of the data and suggested that the variation in the intensity of continuum could be explained

by the hypothesis that the inner portion of the plasma sheet, acting like a rigid disk, might cast a radio shadow at larger radial distances, even though the plasma sheet bends over (at the "hinge point") at large distances to lie approximately in the anti–solar direction. Barbosa assumed that the source region lies at the edge of the plasma sheet Jupiterward of the hinge point at around 30–50 R_J where the plasma frequency is estimated to be ~3 kHz (Barbosa et al., 1979). Leblanc et al. (1986) had eliminated the plasma sheet as a possible source because of the lack of evidence in that vicinity for the existence of ESUH waves which are believed to be the predominant source of continuum. Kurth et al. (1987) in their reply to Barbosa provided further evidence in support of their earlier interpretation, and argued that the data are not well–ordered by Barbosa's model.

Moses et al. (1987) and Kennel et al. (1987) investigated wideband plasma wave data and showed that, on occasions, intense electromagnetic Z–mode emissions exist within the Jovian tail lobes. Without the wideband data such emissions could not have been readily distinguished from nonthermal continuum radiation. Their ability to separate Z–mode from continuum radiation rested mostly on the identification of the emissions' frequency cut–offs: in fact, for the Z–mode to be identified, 0–mode continuum had to be absent. It was therefore concluded that at various times there must be an absence of 0–mode in the continuum but that its presence at other times cannot be ruled out. Indeed Moses et al. (1987) found that, for an event which they studied in depth using wave polarization measurements, the 0 and Z–modes coexisted. At this point in time, therefore, the predominant polarization of Jovian continuum, its source location and even perhaps its source mechanism remain to be identified unambiguously.

3.2 Jovian kilometric radiation (KOM)

The progress in locating the sources of broadband and narrowband kilometric radiation, bKOM and nKOM, has been comparatively rapid since Leblanc and Daigne (1985a) corrected the bKOM polarization results of Desch and Kaiser (1980).

3.2.1 bKOM

Leblanc and Daigne (1985a), in a most comprehensive study of bKOM, confirmed the temporally bursty character of the radiation, its general occurrence in the range 120° – 270° CML as observed by Voyagers (see Figure 8 for a reminder of the Jovian coordinate systems), and its V-shaped envelope on spectrograms as reproduced in Figure 9 (from Desch and Kaiser, 1980). Leblanc and Daigne (1985a) found, however, that the CML range for maximum occurrence changed from a single peak at 150° – 240° CML pre–encounter to two peaks post–encounter – one at 140° and the other, less prominent, drifting from 120° to 270° CML with increasing spacecraft distance. These observations are summarized in Figure 10. Outside the main peaks, at 0° to 120° CML and 300° to 360° CML, there exists what Leblanc and Daigne called an "intermittent emission" (cross–hatched in Figure 10) whose sense of polarization is reversed relative to the "main"emission. From these results it seems clear that the observer's zenomagnetic latitude, which depends on CML (see Figure 8), has an important effect on the occurrence pattern of bKOM and on the observed polarization.

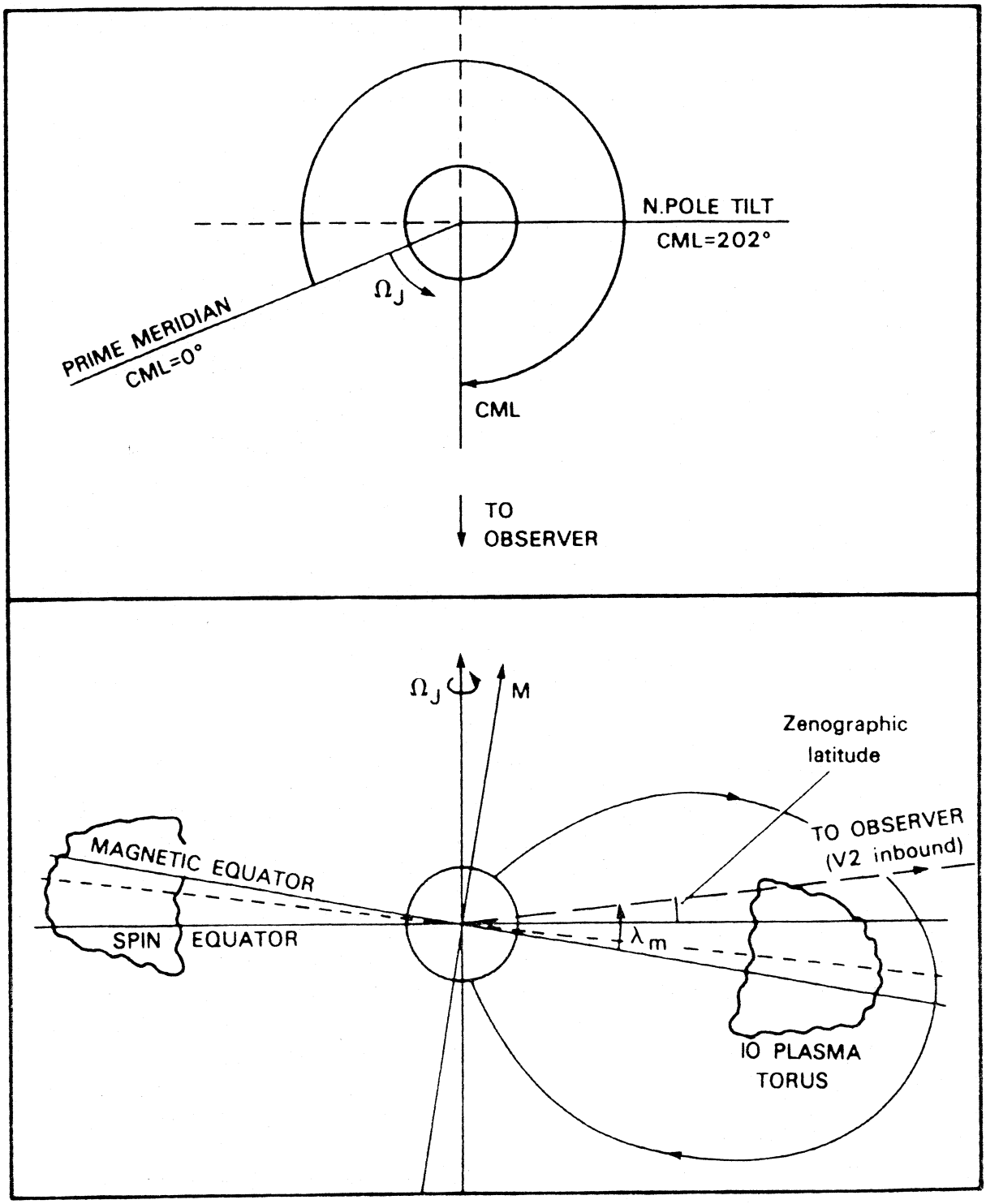

Fig. 8: Upper frame: Jovian coordinate system as viewed from above the north spin pole. The prime Central Meridian Longitude CML = 0° rotates anticlockwise at rate Ω_J. Jupiter's north magnetic pole is tilted 9.6° in direction CML = 202°.
Lower frame: Meridian section at CML = 202° showing north magnetic pole tilted 9.6° towards an observer whose magnetic latitude λ_m = 9.6° + observer's zenographic latitude. As Jupiter rotates λ_m varies sinusoidally.

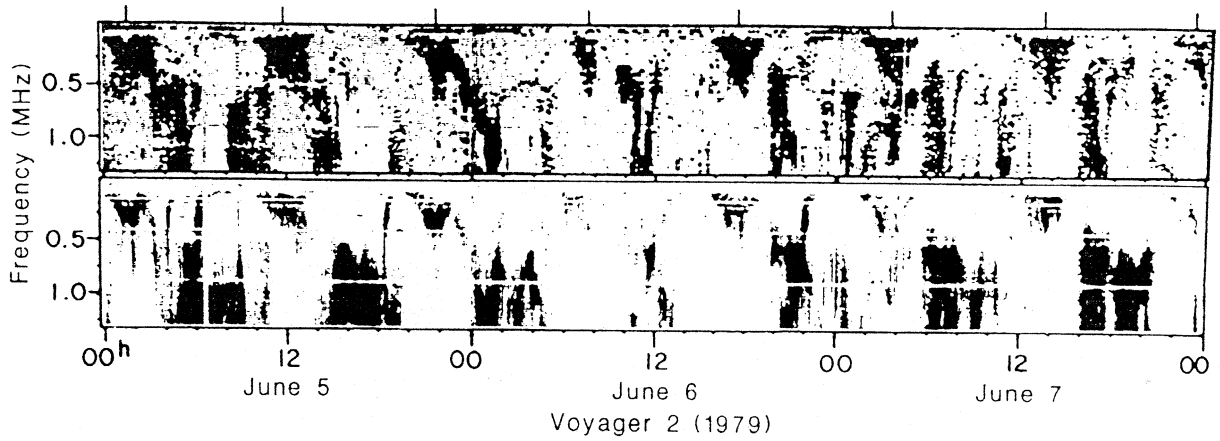

Fig. 9: Voyager 2 spectrogram of Jovian radio emissions in the range 20 kHz – 1.3 MHz (from Desch and Kaiser, 1980). Total power is shown in the bottom panel, increasing darkness proportional to increasing wave intensity. The upper panel shows the polarization of the emissions with black (white) representing RH (LH) polarized emission. In the 72–h period shown, eight consecutive bKOM events are visible as the V–shaped emissions extending up to ∼ 500 – 600 kHz and coincident with the north dipole tip passage (ticks on top axis); their polarization is right–handed.

Without a doubt, one of the most important results by Leblanc and Daigne (1985a), based on a study by Ortega–Molina and Daigne (1984), was the correct determination of bKOM polarization which contradicted the earlier results of Desch and Kaiser (1980) and Alexander et al. (1981) who had not taken into account the difference between the electric and physical planes of the antennae on Voyagers. Hence the polarization of bKOM is now known to be right–handed when observed at northern magnetic latitudes ("main" emission) and left–handed at southern magnetic latitudes ("intermittent" emission). A qualification was added to the latter conclusion; the polarization in the high frequency range could be reversed with respect to that in the low frequency range, the reversal statistically occurring at ∼100 kHz (Leblanc and Daigne, 1985a). It seems that this reversal may sometimes be due to contamination by the presence of Jovian hectometric radiation (Leblanc, private communication) but this deserves further study.

Leblanc and Daigne (1985a) suggested that the beaming of bKOM to the northern and southern hemispheres was due to shadowing, by the Io torus, of emission produced in the X–mode on the *inner* flanks of the torus, at 5–6 R_J. Green and Gurnett (1980) had earlier proposed a similar shadowing, by the torus, of 0–mode emission at frequency f $= 2f_p$, produced above Jupiter's auroral zones, the polarization being compatible with Desch and Kaiser's (1980) results but now incompatible with the corrected polarization. Leblanc and Daigne (1985a) proposed that the lower and higher bKOM frequencies are respectively produced by the maser cyclotron instability as invoked for terrestrial auroral kilometric radiation (Wu and Lee, 1979; Wu et al., 1982) and by the non–linear interaction of electrostatic waves (Roux and Pellat, 1979). The middle frames of Figures 11 and 12 (from Leblanc and Daigne, 1985a) provide an excellent summary of the manner in

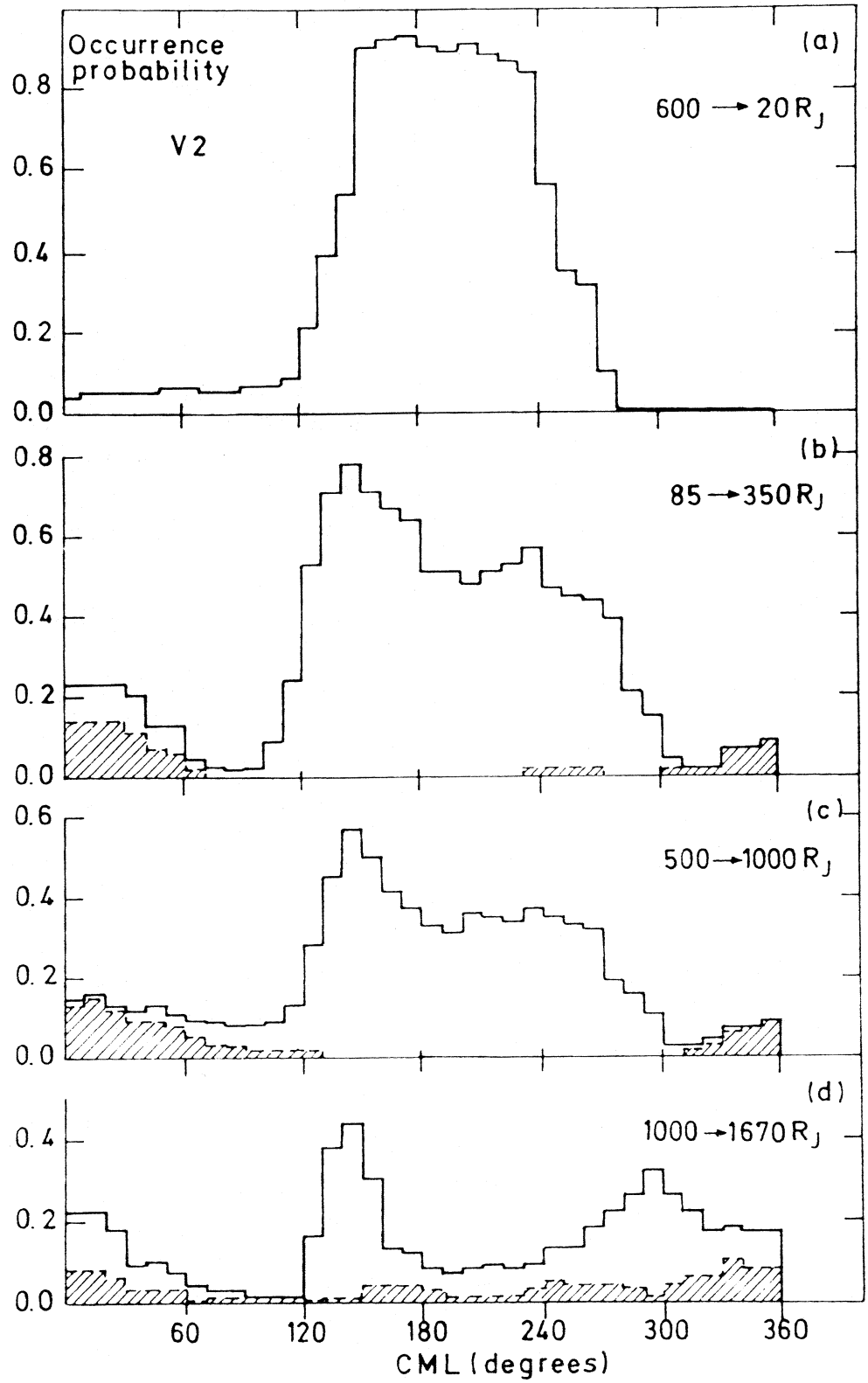

Fig. 10: Probability of occurrence in CML of bKOM emission observed by V1 at different distances from Jupiter. The white histogram refers to the "main" (northern hemisphere) component whereas the shaded area refers to the "intermittent" (southern hemisphere) component, of opposite (LH) polarization (from Leblanc and Daigne, 1985a).

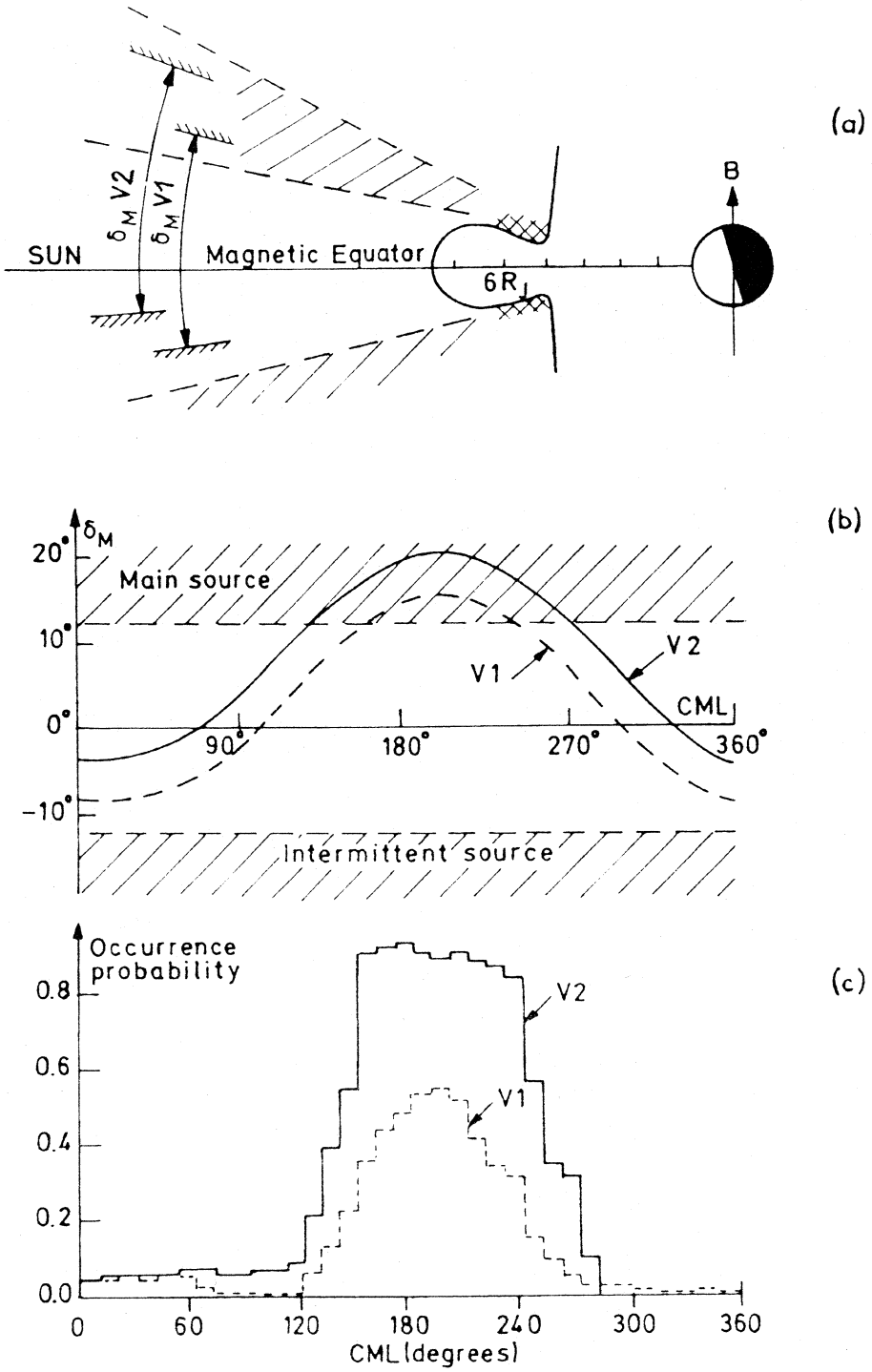

Fig. 11: The source model on the dayside hemisphere according to Leblanc and Daigne (1985a). (a) Beaming of the emission in a meridian plane at a given frequency, the source being assumed to lie at the inner boundary of the Io torus.
(b) A latitudinally fixed observed (on V1 and V2) will be swept into the beam only for given ranges of longitude due to the tilt angle of the magnetic field (δ_m is the observer's magnetic latitude).
(c) The occurrence probability of the bKOM for V1 and V2 pre–encounter observations (600 – 20 R_J).

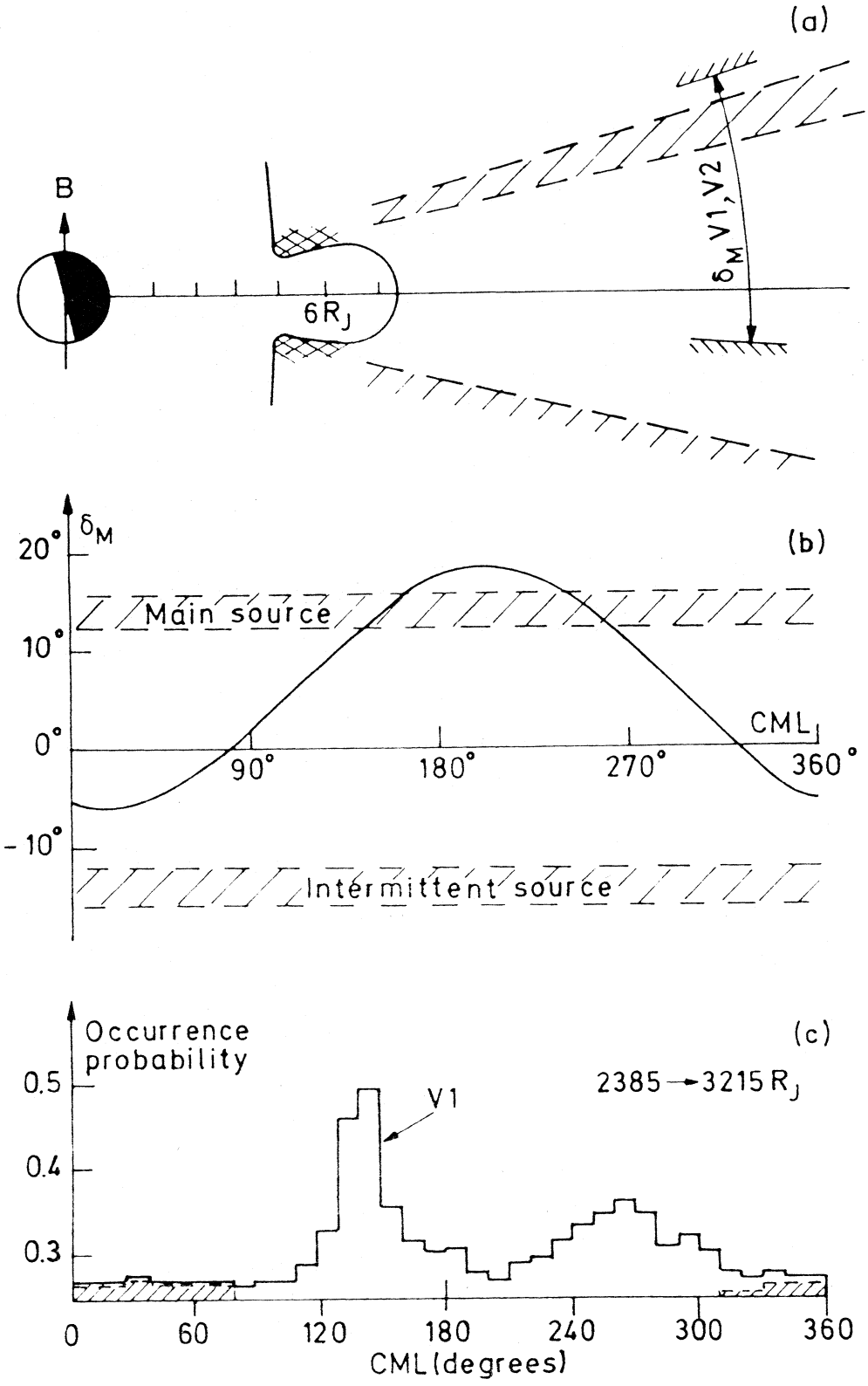

Fig. 12: As for Figure 11 but for nightside, post–encounter, observations on V1.

which bKOM is envisaged to be beamed in latitude on the dayside and nightside of Jupiter. However, it is not clear from the sketches in the upper frames how X–mode radiation, from the hatched source regions suggested, can have the polarization observed by Voyagers. Jupiter's magnetic field lines have a southward pointing component in the proposed source regions; thus X–mode radiation from the northern hemisphere and that from the southern source will be right–handed when observed in the southern hemisphere which is the opposite to what was actually recorded.

Besides the above suggestions by Leblanc and Daigne (1985a), two other theories have been proposed for the source mechanism and location of bKOM. That of Green and Gurnett (1980) has already been mentioned; it required bKOM to be somehow produced as $2f_p$ emission in the 0–mode from the auroral zones. They performed ray–tracing to show how the Io plasma torus could act as an obstacle to propagation close to the equatorial plane, thereby resulting in "beams" of bKOM in the north and south hemispheres beyond the torus. The polarization of these beams would respectively be left–handed and right–handed which is, again, the opposite to what was observed. Therefore this theory does not appear to have been pursued further in the literature, although it seems that theoretical efforts are being made to reverse somehow the polarization along the propagation path in an endeavour to make the polarization fit the observations (M. Desch, private communication).

The other theory, by Jones (1980; 1981a) contained the proposal that the beaming was inherent to the generation mechanism, with the source located on the outer flank of the Io torus near the magnetic equatorial plane. This theory, the linear mode–conversion window (LMCW) theory, is the same as that proposed for terrestrial myriametric radiation (TMR) (Jones, 1980; 1981b) which was described in some detail earlier, in Section 2. Electrostatic upper–hybrid (ESUH) waves are again considered to be the source, with their propagation in the density gradients of the Io torus ultimately resulting in emission in the 0–mode. Intense ESUH waves were consistently observed within 23 R_J of the planet (Warwick et al., 1979a; Gurnett et al., 1979b) which were confined to within 1.9° of the magnetic equatorial plane (Barbosa and Kurth, 1980) except in the Io torus itself where they covered a larger latitude range. As for TMR, the ESUH waves, by virtue of their propagation in a density gradient normal to the magnetic field, first become Z–mode waves which, in turn, after further propagation in the Io torus, convert into 0–mode radiation through radio windows which exist where the wave frequency equals the plasma frequency $f_p = 9 \cdot 10^3 N_e^{1/2}$ kHz, where N_e [m^{-3}] is the electron concentration. On passing through the radio windows into the low–density region outside the torus, the 0–mode radiation emanates as two beams at angles $\beta = \pm \arctan(f_p/f_c)^{1/2}$ with respect to the magnetic field line at the window location, $f_c = 0.028$ B kHz being the electron cyclotron frequency for a magnetic field strength of B [nT]. Thus, as was shown for TMR, for a source at the equatorial plane in a dipole magnetic field, the radiation is beamed at angles $\alpha = (\pi/2 - \beta)$ to the equatorial plane, one beam to the north and one to the south. If the emitting region is distributed about the equatorial plane by $\sim \pm 2°$ as would be the case if the Jovian ESUH waves on the outer flank of the Io torus are the source, then the southern edge of the northern beam would be expected to derive from the most southerly element of the source, that is from

–2° magnetic latitude. Typical ray paths derived from ray–tracing calculations in a dipole magnetic field and a fairly realistic torus model which clearly illustrate this configuration have been shown in Figure 2 of Jones (1981a); Figures 15 and 16 here contain similar information. Had Voyagers' excursions in magnetic latitude been greater then, according to the theory, they would have observed the high latitude edges of the beams which, in the case of the northern hemisphere beam, would have derived from the most northerly source, that is from +2° magnetic latitude. This effect, where Voyagers appeared to pass right through the beams, has been observed on both Voyager 1 and 2 when outbound on the nightside as can be seen from Figures 10 and 12, despite Voyagers being at lower Jovicentric latitudes ($\sim 5°$) than for V2 inbound (7.2°). This would imply that the beams make smaller angles to the magnetic equatorial plane and have a smaller width, possibly due to a smaller latitudinal source dimension. Figure 12 would illustrate these points had the beam locations in Figure 12b been correctly located at $\delta_M \simeq \pm(9° - 12°)$ to coincide with the peaks in the occurrence probability plot in Figure 12c.

If the LMCW theory is valid for bKOM, then the emission will occur at the plasma frequency f_p at angles $\beta = \pm \arctan(f_p/f_c)^{1/2}$ with respect to the magnetic field line. Thus, assuming a source position at radial distance R_s and magnetic latitude λ_{ms}, the magnetic field magnitude and direction at that point can be computed (Connerney et al., 1981).

Furthermore, assuming a value for f_p within the range of bKOM frequencies observed by Voyager, the theoretical direction of the beam at this frequency can also be computed. If the beam does not intersect the position at where the spacecraft lies when that particular bKOM frequency is observed, then the assumed source location is incorrect and another value of R_s is tried until one iterates onto a location that fits. If this technique is applied for all the bKOM frequencies within a tapered emission, using the corresponding positions of Voyager when they are observed, a radial profile of f_p and therefore N_e in the Io torus can be constructed. As was mentioned earlier, the "remote–sensing" technique has been applied to TMR with considerable success, it being assumed that the Earth's magnetic field is dipolar within about 4 R_E. Jupiter's magnetic field near equatorial plane at the Io torus and beyond is complicated by the presence of the equatorial current sheet as shown in Figure 13 (from Connerney et al., 1981). In this figure is shown a comparison of model magnetospheric field lines, using Voyager 1 data, with dipole field lines. The values on the field lines indicate the equatorial distance of field line crossing in the absence of the magnetodisc current sheet.

Jones (1986a) and Jones and Leblanc (1987) used Voyager 2 inbound data in their remote sensing because the spacecraft's higher latitude resulted in excursions in and out of the northern beam during a relatively large number of consecutive Jovian rotations. As was stated earlier, it was assumed that the southern edge of the northern bKOM beam derives from a source at $\lambda_{ms} = -2°$. The positions of V2 were determined when the leading edge of bKOM at different frequencies (see Figure 9) was observed, the CML of the spacecraft at this time being $< 202°$ CML. These V2 positions were determined for nine consecutive Jovian rotations when V2 was inbound from 95 R_J to 55 R_J, and the Io

torus plasma concentration profiles obtained by the remote–sensing technique are shown in Figure 14a. Also shown, for comparison, are the profiles determined *in situ* by two experiments (Barbosa and Kurth, 1980; Bagenal et al., 1985) on V1 which had traversed the torus 4 months previously. The remotely–sensed profiles are remarkably consistent within themselves considering that there must have been temporal variations in the torus during the 5 days involved, during which Io made nearly three rotations around Jupiter. The anomalous results at the lowest density were attributed to a wave refraction effect between the source and the spacecraft, which could be important at low frequencies.

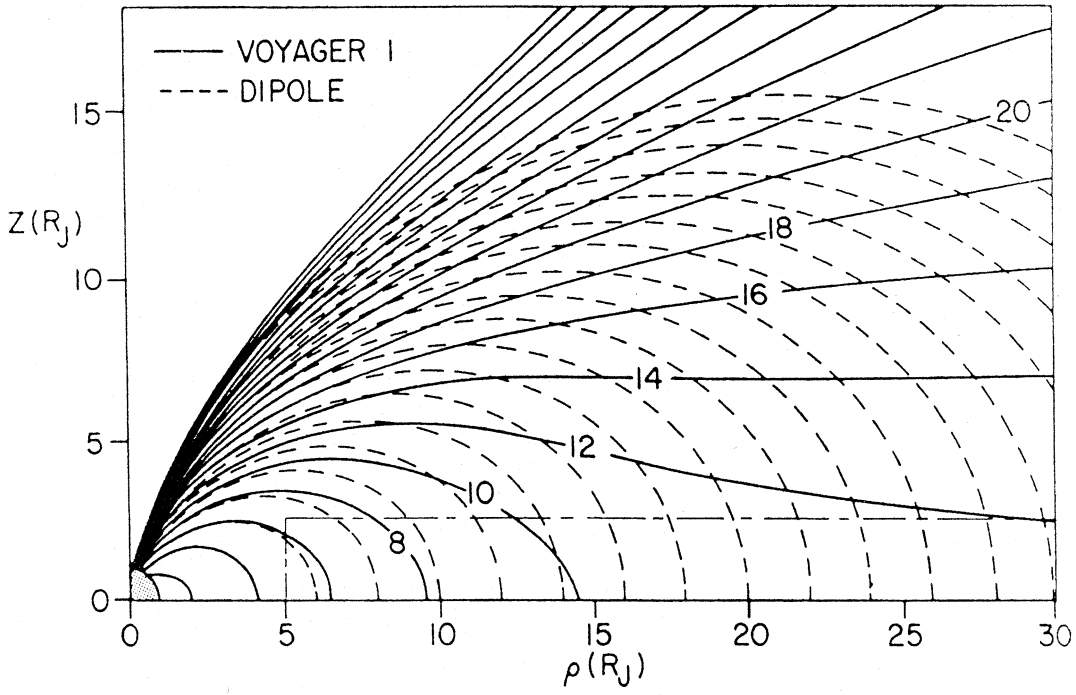

Fig. 13: Meridian plane projections of magnetospheric field lines (heavy) as determined from Voyager 1 data, and of dipole field lines (dashed). Values on field lines indicate equatorial distance of field line crossing in absence of magnetodisc current sheet (from Connerney et al., 1981).

The same remote–sensing exercise was performed using the trailing edge of the same bKOM emissions, again observed in the northern hemisphere but with V2 moving down in magnetic latitude towards the equatorial plane. Figure 14b shows the profiles obtained for a source latitude of $\lambda_{ms} = -1°$ which was found to yield a better agreement with the *in situ* profiles than $\lambda_{ms} = -2°$. This difference was attributed to small differences in the widths or positions of the source regions with CML since Figure 14b corresponds to CML $> 202°$.

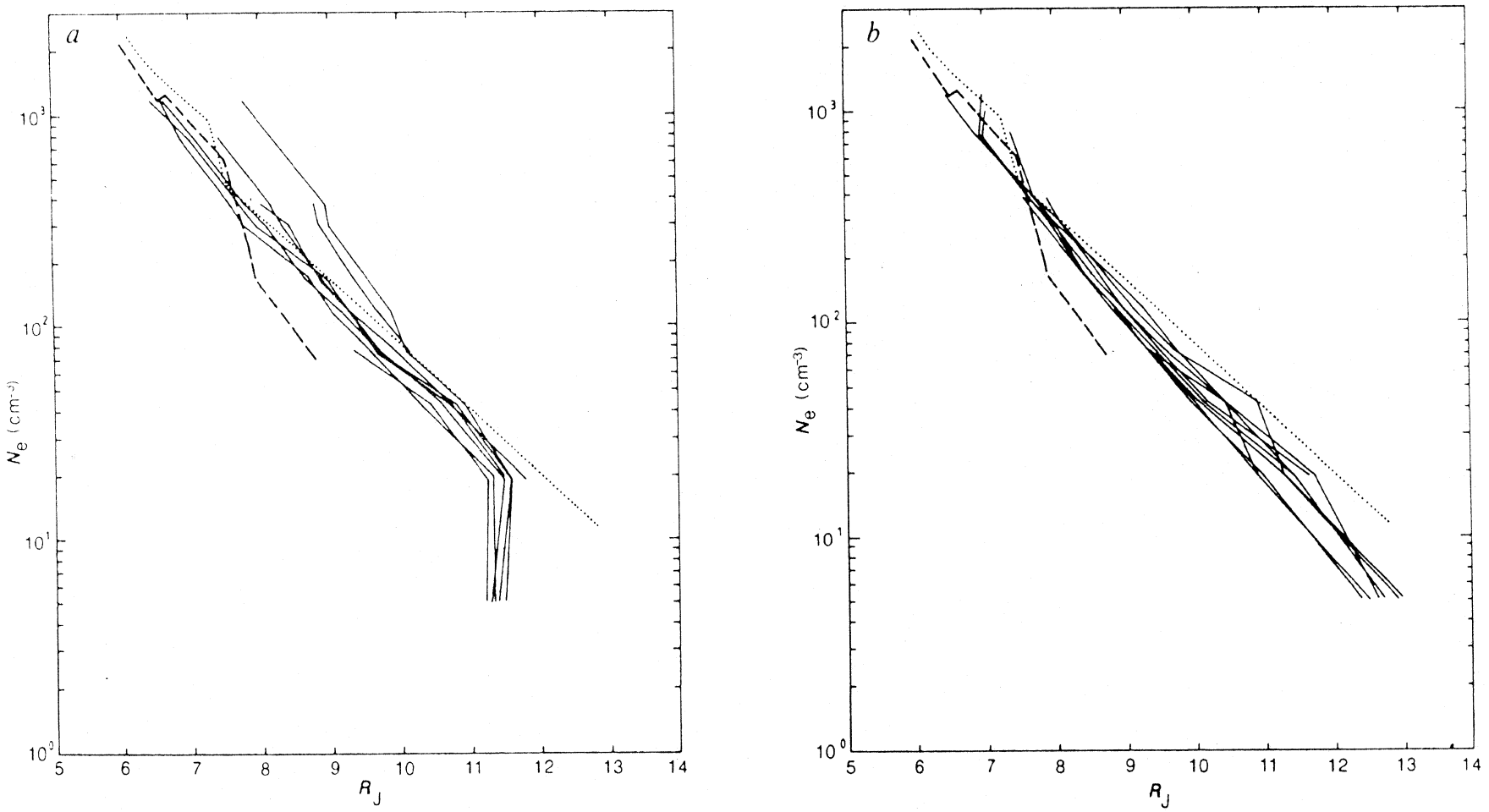

Fig. 14: (a) Plasma density profiles of the Io torus obtained by remote sensing using the start times of bKOM observed during nine Jovian rotations when Voyager 2 was inbound from 95 R_J. All sources are assumed to be at magnetic latitude $\lambda_{ms} = -2°$. The dashed line represents the profile determined from in situ Voyager 1 measurements by the plasma science PLS experiment (Bagenal et al., 1985) and the dotted line is derived from measurements of the upper hybrid frequency by the planetary radio astronomy PRA and plasma wave system PWS experiments (Barbosa and Kurth, 1980).
(b) As for (a), but using the end times of bKOM and assuming all sources are at magnetic latitude $\lambda_{ms} = -1°$.

In both Figures, 14a and b, the slopes of the remotely–sensed profiles differ only slightly from that of the *in situ* profile determined from the observations of upper hybrid waves (dotted line) (Barbosa and Kurth, 1980). Jones (1986a) states that if one had assumed that the latitudinal extent of the source decreased by $\sim 0.5°$ with increasing distance from 8 R_J to 13 R_J, the slopes would be identical. A decrease in width of ESUH emission regions with distance was observed by Kurth et al. (1980a).

To demonstrate the converse of the above results, namely how the tapered emissions of the type shown in Figure 9 are formed by LMCW emission from the Io torus which has a profile similar to those in Figure 14b, one profile is selected and the bKOM beam directions at the different PRA frequencies computed. The profile used is shown in the lower portion of Figure 15 with the bKOM beams in the upper portion. It is clear from the latter that a spacecraft moving upwards to higher latitudes would observe the higher frequencies later; when the spacecraft moves downwards from its highest latitude, the higher frequencies would disappear first. Hence the receiver records a tapered emission.

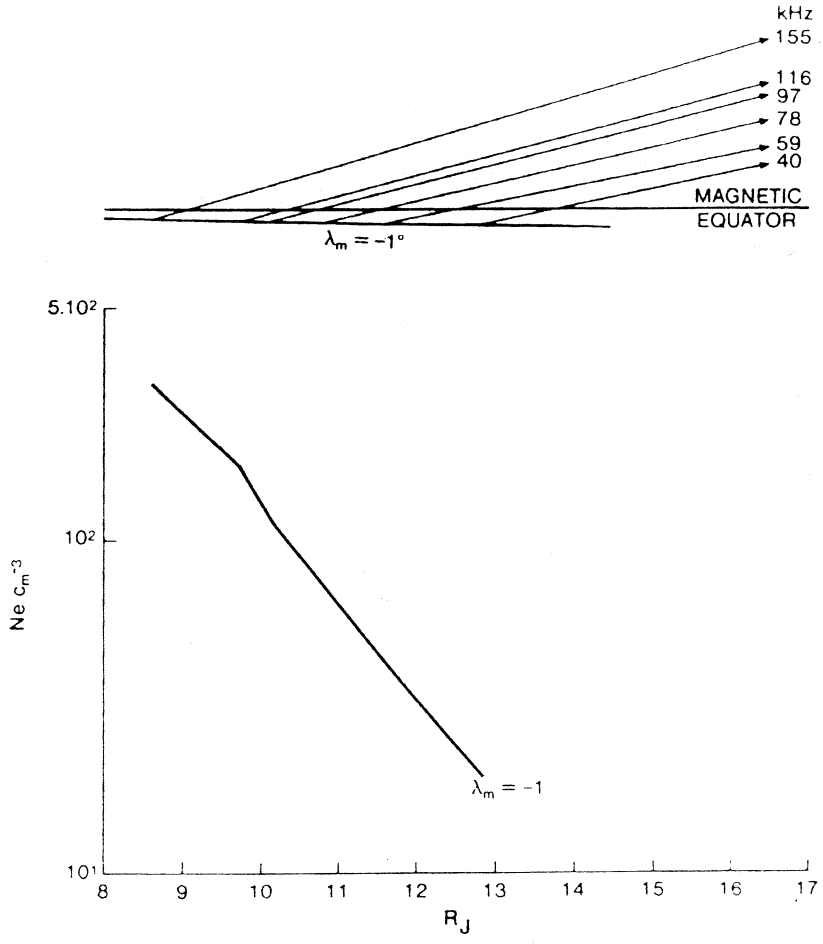

Fig. 15: Lower: One of the profiles from Figure 14b. Upper: Beams of bKOM from sources at $\lambda_{ms} = -1°$ for the profile shown in the lower panel.

Because the beam widths depend, to a first approximation, on the latitudinal dimensions of the source, as illustrated in Figure 16, computations show that for V2 to have observed the top edge of the northern beam when inbound on the dayside, the source would have had to be restricted to within $\lambda_{ms} \sim 0.5°$ of the equatorial plane and even then the effect would have been visible only at the higher frequencies. Alternatively, had Voyager 2's excursion into the northern hemisphere been greater than $\lambda_m \simeq 20 - 25°$, it would have observed the whole beam at all frequencies (Jones, 1986a).

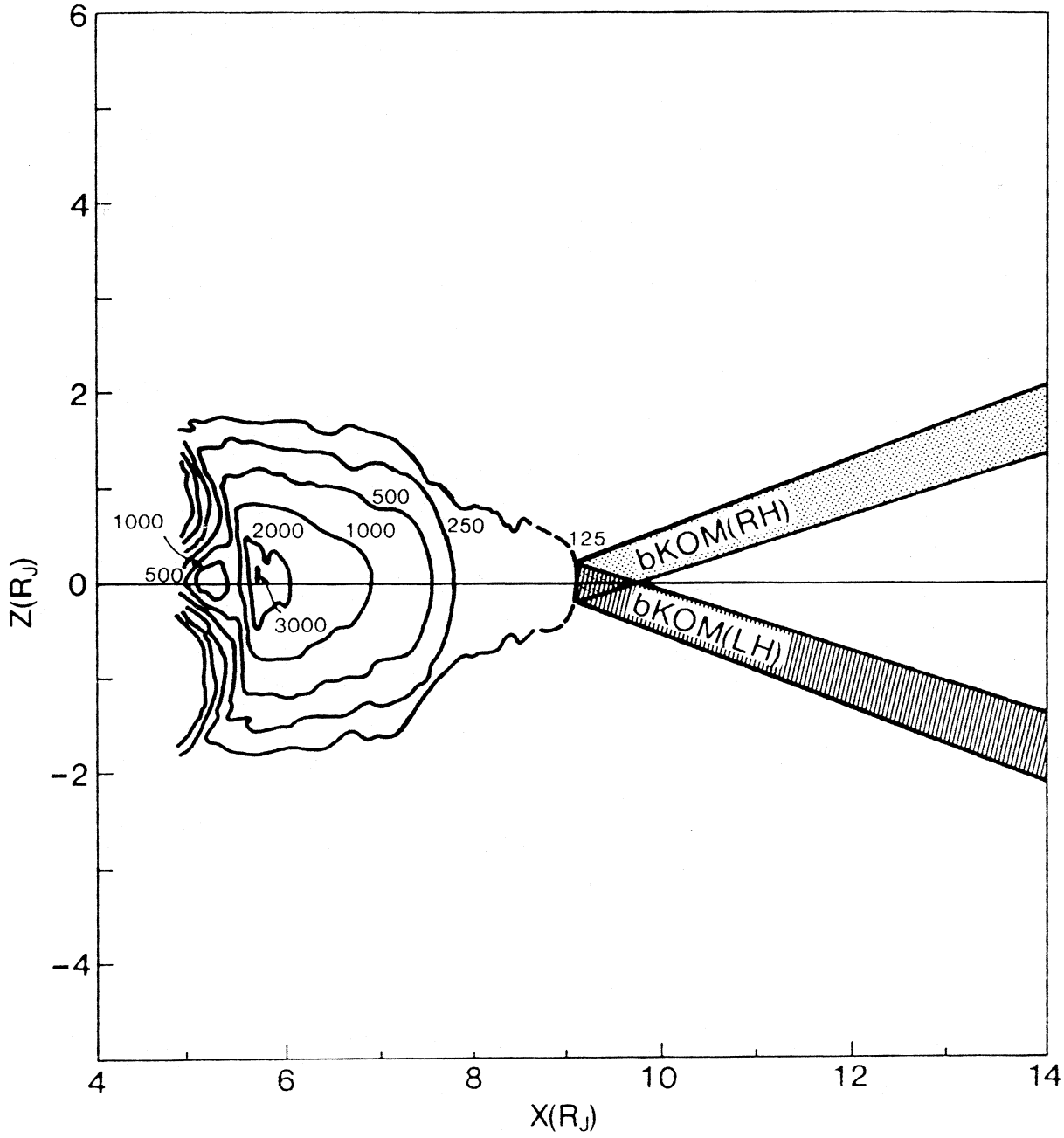

Fig. 16: Schematic of bKOM (100 kHz) beaming from the Io plasma torus (Bagenal et al.'s (1985) torus model); the contours are labelled according to plasma density (cm^{-3}).

Figure 16 summarizes the salient conclusions obtained by applying the LMCW theory to the production of bKOM. The Io torus plasma density contours are obtained from Bagenal et al. (1985); a density of 125 cm^{-3} corresponds to a plasma frequency, f_p, of 100 kHz. Thus the source shown corresponds to f_p = 100 kHz, which is the bKOM emission frequency; the source is assumed to be 3° wide, from –1.5° to 1.5° in magnetic latitude. The northern beam's polarization is right–handed (RH) whereas the southern's is left–handed (LH) which is as is observed. It should be noted that near the magnetic equator the density gradient would be expected to be nearly normal to the magnetic field lines (see Figure 13) which is a necessary condition in the LMCW theory.

Jones (1986a) states in his conclusion that, bearing in mind the temporal and longitudinal variations of the torus plasma density and of the current sheet magnetic field which was assumed constant, it is difficult to imagine that the remotely–sensed profiles obtained using data from a spacecraft more than $3 \cdot 10^6$ km from the source could be so consistently similar to the in–situ profiles unless the LMCW theory is valid.

3.2.2 nKOM

The first observations of nKOM were made when Voyagers were within 0.7 AU of their encounter with Jupiter (Warwick et al., 1979a). It is generally confined to 60 – 150 kHz, with bandwidths typically 40 – 80 kHz, although some events are seen at 20 kHz and 250 kHz and with bandwidths < 20 kHz (Kaiser and Desch, 1980; Leblanc, this volume). Figure 17 (from Kaiser and Desch, 1980) shows wave spectrograms from V1 before encounter at a radial distance of 160 R_J. The lower panel shows nKOM as narrow (black) bands at ∼100 kHz; the separate emissions at higher frequencies are Jovian hectometric radiation. The upper panel displays the sense of polarization of the emissions. The polarization of nKOM has also been surrounded by some confusion. Kaiser and Desch (1980) reported that nKOM observed by Voyagers in the northern and southern hemispheres were respectively left–hand and right–hand polarized, but this conclusion was later reversed by Kaiser and Desch (1984). In another detailed study of nKOM, Daigne and Leblanc (1986) showed that the former conclusion was correct and thus, as observed by Voyagers, nKOM has the opposite polarization to bKOM. For the nKOM in the upper panel of Figure 17, black therefore represents left–hand polarization.

It is clear from Figure 17 that nKOM is beamed such that the emission is predominantly observed when the north magnetic pole is tilted towards or away from the spacecraft. This is shown clearly in Figure 18 (from Daigne and Leblanc, 1986) where the occurrence probability of nKOM appears as a function of CML. Note again that the polarization reversal from right–handed (RH) to left–handed (LH) occurs near to, but not exactly at, where the spacecraft cross the magnetic equator ($\delta_M = 0°$).

There have been a number of suggestions that nKOM derives from the Io plasma torus (Warwick et al., 1979b; Jones, 1980; Kaiser and Desch, 1980). The electron plasma frequency f_p and the upper–hybrid frequency f_{uh} in the torus at 8 – 9 R_J are ∼100 kHz, similar to the frequency of nKOM. Also, long–lived nKOM which reappeared for many consecutive Jovian rotations sometimes showed a 3 – 5 % lag from co–rotation which was

taken as being suggestive of plasma–loading effects (Hill, 1979; 1980) at distances beyond the Io orbit (Kaiser and Desch, 1980). Further, the observation of nKOM relatively close to the torus restricts the position of the source to the outer torus because of shadowing by the torus for waves propagating from locations closer to Jupiter.

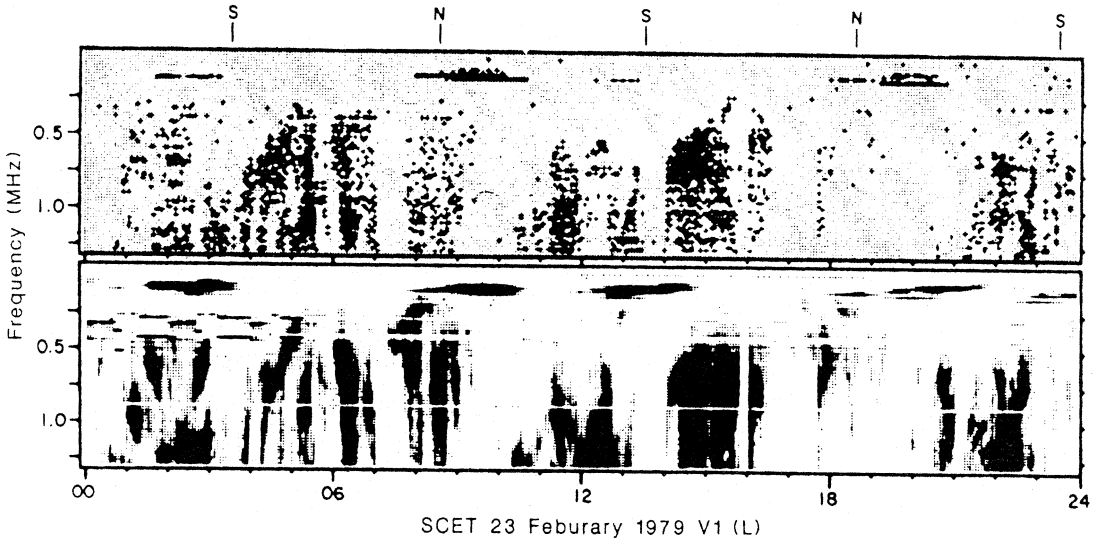

Fig. 17: As for Figure 9 but showing nKOM with V1 inbound at a distance of 160 R_J from Jupiter (from Kaiser and Desch, 1980). The nKOM emissions are seen in the lower panel as relatively dark lines at ∼100 kHz. The upper panel shows the corresponding nKOM polarization, black (white) being left (right) handed, the opposite to Figure 9.

Only two theories have been proposed for the production of nKOM. The linear mode conversion window (LMCW) theory (Jones, 1980; 1987b) invoked the same mechanism as for bKOM generation, the nKOM source being found, by remote–sensing, also to lie in the Io torus, but at latitudes greater than $\sim \pm 8°$, i.e. away from the equatorial plane. The reasons for arriving at these source locations will be given later. A non–linear theory by Fung and Papadopoulos (1987) (henceforth referred to as F & P) invokes an up–conversion interaction of ESUH waves in the Io torus, as Roux and Pellat (1979) suggested for terrestrial auroral kilometric radiation, the resulting electromagnetic emission being at a frequency 2 f_{uh} in the X–mode (Fung, 1985) or O–mode (F & P). F & P, as did Kaiser and Desch (1980), locate the nKOM sources in the Io torus at 7.5 – 9 R_J. They assume a dipole magnetic field and, in the example they present, their theory requires the density gradient to be at an angle of 47° with respect to the magnetic field; furthermore, the ESUH waves need to be at a level of ∼10 V/m in order for the pump depletion they invoke to produce the observed power and O–mode polarization. They do claim however that their Figure 11, a plot from Bagenal and Sullivan (1981) showing "total ions per unit L shell" versus "radial distance", strongly suggests that the proper orientation of the local density gradient exists near 7.5 – 9 R_J. It is difficult to comprehend how this conclusion is arrived at since their Figure 11 does not contain the required directional information. At this stage, therefore, it is difficult to assess the credibility of this theory, which also seems to be the case for the non–linear theories for TMR production. It is necessary for

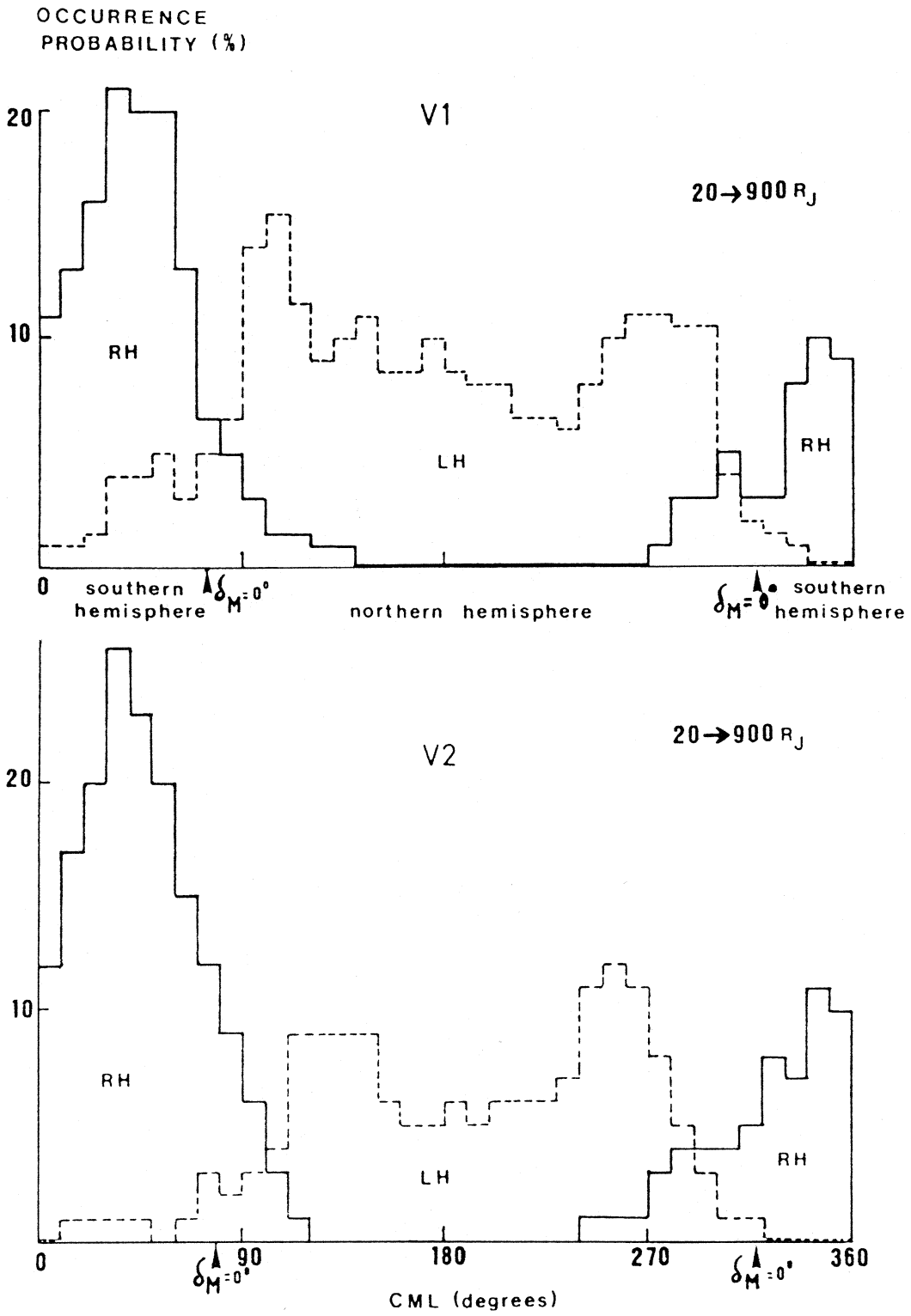

Fig. 18: Occurrence probability of nKOM events with CML, as observed after encounter by V1 (top) and V2 (bottom) (from Daigne and Leblanc, 1986). The dipole magnetic equator crossings are indicated by arrows ($\delta_M = 0°$). The emission is right–hand (RH) polarized when seen in the southern hemisphere and left hand (LH) polarized when observed in the northern hemisphere.

the proponents of these theories to propose predictions which can be tested by existing or future observations.

The linear mode–conversion "window" (LMCW) theory, which seems to be able to explain the generation of TMR (Jones et al., 1987) and bKOM (Jones, 1986a), has also been applied to nKOM (Jones, 1987b). As was mentioned previously, the LMCW theory predicts the beaming of radiation at angles $\beta = \pm \arctan \sqrt{f_p/f_c}$ relative to the source/window magnetic field vector. As explained in the discussion of bKOM, this allows remote–sensing of the sources in a model magnetic field and some results using this technique are shown in Figure 19 (from Jones, 1987b). These were obtained by determining the magnetic coordinates of V1 when the various frequencies constituting the nKOM in Figure 18 started and ended. If the nKOM is produced according to the LMCW theory, these times and positions would correspond to V1's entry into, and exit from, the beam. Source latitudes up to the limit of the Io torus were assumed to be possible and the radial positions of the sources satisfying the remote–sensing equation were computed. The results for f = 78 kHz are shown in Figure 19.

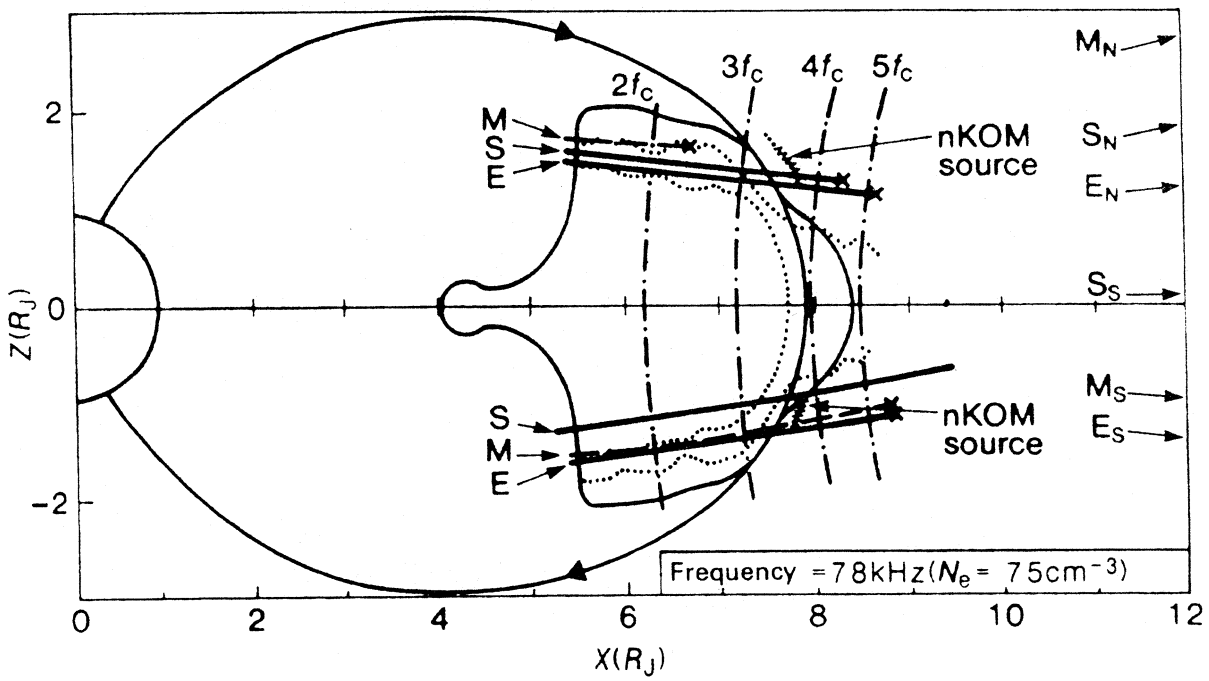

Fig. 19: Remote–sensing results of 78–kHz nKOM sources overlaid on isodensity contours in the Io plasma torus. The heavy, full lines labelled S (start) and E(end) constitute possible source locations of the start and end of the emissions observed by V1. When the start and end of the northern emission were observed, V1 was at the latitudes denoted by S_N, E_N respectively. The corresponding latitudes when observing the southern source limits are denoted S_S and E_S. M_N and M_S show latitudes in between when the possible source locations marked M were computed. The nearly vertical lines depict where the cyclotron frequency f_c = 78 kHz/n where n = 2,...,5. The probable nKOM sources lie at the locations shown.

When V1 was moving south at latitude 0.9° at 01:30 Spacecraft Event Time (SCET) on 23 February 1979 (see Figure 17) it entered the 78 kHz beam from the southern source; the spacecraft latitude is indicated by the arrow marked S_S (Figure 19, right). The end of the event occurred when V1 was at its most southerly latitude, – 6.4° (E_S in Figure 19). The emission observed between these two locations consisted of a fairly broad peak, intensity increasing and decreasing fairly smoothly as the spacecraft moved from S_S to E_S; the maximum signal was recorded at the position marked M_S although it was little greater than other maxima within the main emission. The nearly horizontal lines in the southern half of the Io torus labelled S, M and E are the corresponding loci of possible source positions as obtained by remote sensing.

The same procedure was applied to many other events and the source loci for the northern beam for the event before that above are shown in the northern half of the torus in Figure 19. The maximum signal was recorded near the spacecraft's most northerly position (M_N) which may indicate that V1 had not reached the maximum within the beam. Taking into account that the crosses on the loci in Figure 19 indicate the maximum radial distance at which, according to the theory, a source of the correct polarization is visible to V1, and that the 78 kHz contour in the torus, as determined in situ by V1, is as shown, the most likely sources of nKOM lie at ∼8 R_J at 8 – 12° and 7 – 10° in the northern and southern hemispheres respectively. In these regions the source–ESUH waves at 78 kHz (at $f_{uh} = \sqrt{f_p^2 + f_c^2} = 78$ kHz) lie between the third and fourth (or fourth and fifth) harmonics of f_c. It is well known that the intensity of ESUH waves maximizes at $\sim (n + 1/2)f_c$ and that they suffer cyclotron damping at nf_c. Remote sensing using other frequencies (97 – 154.8 kHz) for these and other nKOM events show similar results.

Near the suggested source locations the magnetic field line appears nearly parallel to the isodensity contours as modelled from in situ measurements; as already stressed, this is a condition required by the linear mode conversion mechanism (∇N_e normal to B_0). With the available models, at no other point in the outer torus does this condition appear to be satisfied except near the equatorial plane where the bKOM sources are believed to be located (Jones, 1986b). If nKOM sources are in the positions shown, many of the radiation's characteristics can be readily explained.

The lower intensity of nKOM compared to bKOM may be attributed to the lower intensity of ESUH waves away from the equatorial plane. Although ESUH waves were detected over a relatively large latitude range in the Io torus, they were not as intense as those seen near the magnetic equator (Barbosa and Kurth, 1980).

Given the existence of the ESUH waves, the frequency of nKOM would be expected to be the plasma frequency where there is a density gradient and where the condition of normality, $\nabla N_e \perp B_0$, is satisfied. It is seen from in situ measurements that the plasma frequency in the suggested source locations is ∼100 kHz which is the approximate frequency of nKOM. Variations of this frequency would occur due to temporal and spatial variations of plasma density in the corresponding torus region. The total bandwidth of nKOM would be expected to correspond to the range of upper–hybrid and plasma frequencies in the source region. If this bandwidth were larger than f_c, nKOM would

itself consist of one or more narrow band emissions corresponding to $f_{uh} \simeq (n + 1/2)f_c$. It appears that, at the source, $f_c \simeq 20$kHz which would result in a minimum bandwidth of ≤ 20 kHz in agreement with observation. It should be noted that the PRA receiver (Warwick et al., 1977) consists of a number of 1–kHz bandwidth filters spaced 19.2 kHz apart, set at frequencies 20.4, 39.6 kHz and so on. Therefore, any fine structure in nKOM with a 20–kHz spacing would not have been resolved. Indeed it is conceivable that on occasions no signal would have been recorded in any of the PRA receiver channels since the emission's frequency bands would have lain between filters.

The computed source locations also explain the smooth temporal nature of nKOM in contrast with the sporadic character of bKOM. Even allowing for variations in f_p in the nKOM source regions, the source–ESUH waves have a fairly wide frequency range (≤ 20 kHz) in which to exist without being damped. It is plausible that the 78–kHz emission region in Figure 19 for example, remained within the $3f_c$ – $4f_c$ band during the period of observation. The sources of bKOM at corresponding frequencies lie in regions (Jones, 1986b) where $f_{uh}/f_c \rightarrow 10$, so that relatively small fluctuations in plasma density (three times smaller in percentage terms) would cause the frequency f_{uh} often to wander between cyclotron harmonic bands resulting in the disappearance of bKOM when $f_{uh} = nf_c$ and its reappearance when $f_{uh} \neq f_c$

The polarization of nKOM observed by the Voyager spacecraft agrees with that expected for the nKOM sources shown. There are cases when the polarization reversal does not occur exactly at the magnetic equator (Kaiser and Desch, 1980; Daigne and Leblanc, 1986); one such case is shown in Figure 19 where the southern, right–handed source is first observed just north of the equatorial plane. This could be due to asymmetries in the plasma torus, either locally or due to the small angle ($\sim 3°$) between the magnetic and centrifugal equatorial planes, the latter being considered to be the symmetry plane of the Io plasma torus (Dessler, 1983).

One observation not explained by the above investigation is the apparent lag of some long–lived nKOM sources relative to co–rotation and the absence of such an effect in bKOM sources which, because of their greater radial distance, should be more susceptible to mass–loading. It may be that the effect is easier to observe in nKOM because of its smoother nature. It may also be an artefact due in some way to the PRA experiment's limitation in being able to observe only certain nearly harmonically related frequencies. The latter may in fact explain why some nKOM sources disappear but later reappear at the correct phase, their disappearance possibly being due to the nKOM frequencies falling between PRA filters as explained earlier. This implies that either the source gradient is changing or that it is moving radially, either out or in. The latter would change the nKOM beaming, an inward motion causing the beams to be dipped to lower latitudes. This would appear as a shift in CML for Voyager observations, but this shift could be either forwards or backwards. Although it seems to be true that the lag is not always present, nKOM more often showing co–rotation (Daigne and Leblanc, 1986), there is no record of nKOM leading co–rotation.

The observed nKOM lag has been the subject of some considerable controversy over the

years. Although it may be reasonable to expect plasma slippage as the radial distance from Jupiter increases (Hill, 1979; 1980), it is most difficult to explain the continued integrity of nKOM sources for numerous rotations (Dessler, 1985; V.Vasyliunas, private communication). Dessler (1985) states that the nKOM must be tied to a surface magnetic feature of the Jovian magnetic field. Simple slipping of a longitudinally uniform distribution of plasma in the torus and outer magnetosphere would not lead to the observed longitudinal persistence of the radio emissions with a 3% longer period. If the nKOM were generated by some chance longitudinal variation in either the number density, temperature, or current flow in the torus, one would expect radial diffusion or radial out–flow to destroy the source region in just a few planetary rotations (Siscoe and Summers, 1981; Hill et al., 1981; 1982; Summers and Siscoe, 1982). Instead, the longitudinal persistence of the nKOM source is reported to continue for at least 40 – 50 rotations (Kaiser and Desch, 1980).

In order that a specific volume of torus plasma maintains its identity while increasing its System III longitude by approximately 11° each rotation, it must be continuously renewed by contact with some magnetic feature associated with the planet that rotates 3% slower than System III. The interpretation of Dessler (1985) and Sandel and Dessler (1988) is that there is a magnetic anomaly at high magnetic latitudes which lags co–rotation and it is the effect of this which, when traced along field lines to the Io torus, causes the nKOM lag. From Connerney et al.'s (1981) magnetic field model, the magnetic latitude at Jupiter of the field–line threading the nKOM source locations in Figure 20 is $\sim 68°$. For the nKOM to display a lag but not bKOM, whose source appears to extend from 7 – 13 R_J at the equatorial plane (see Figure 14) requires a magnetic anomaly at Jupiter very limited in magnetic latitude; in fact, from the results in Figure 14, bKOM at f $\simeq$160 kHz derives from 8 R_J which lies close to the nKOM source field line. It is possible that a lag appears in bKOM at this frequency and this requires investigation. It is also possible that no lag appears in bKOM because the magnetic field at the equator is dominated by the equatorial sheet and that the effect of a localized magnetic anomaly is smeared out.

Figure 20 is a summary by Jones (1987b) of the locations of nKOM and bKOM (78 kHz) sources at the Io torus, and the polarized beams of radiation expected from them. Also shown is the proposed trajectory of Ulysses, a spacecraft which in the next decade is intended to investigate the Sun and solar wind at high ecliptic latitudes. Its Radio and Plasma Wave Experiment (Stone et al., 1983) should allow the first observations of the high–latitude northern hemisphere, right–hand polarized nKOM beam.

3.2.3 Jovian narrowband electromagnetic emissions

This short sub–section is devoted to Jovian narrowband electromagnetic emissions observed by Gurnett et al. (1983b) in Jupiter's magnetospheric cavity. It now seems that these emissions appear as clusters or arcs of narrowband emissions whose frequencies sometimes change gradually with time (W.S. Kurth, private communication). The change in frequency may, in some cases, be related to the magnetic latitude of Voyagers. Efforts are being made to determine, by remote–sensing, the source locations of the emissions, on the assumption that they are produced according to the LMCW theory.

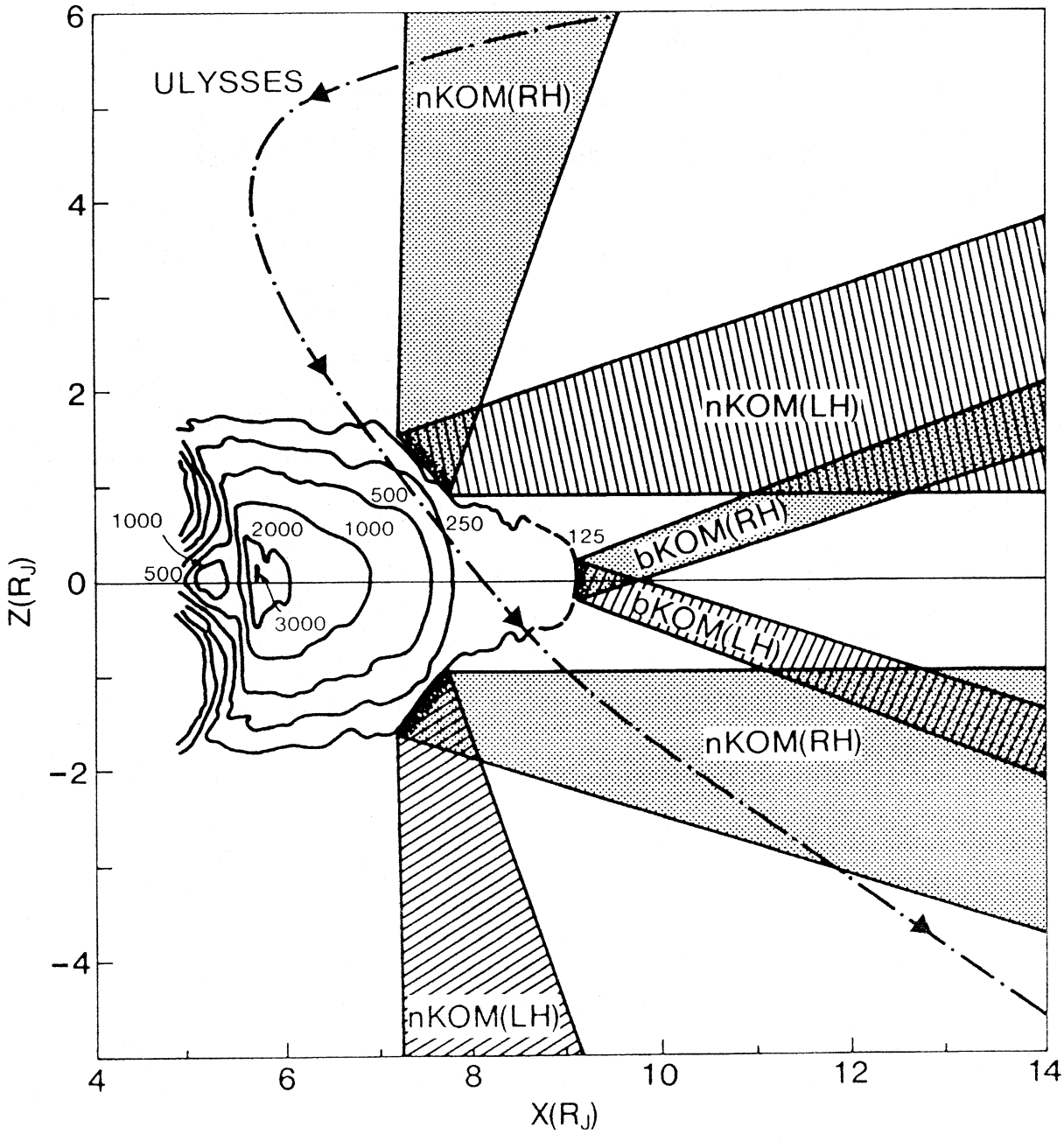

Fig. 20: Summary picture showing examples of the proposed nKOM and bKOM 100 kHz sources. The various beams are sketched and their polarizations indicated. The chained line shows the predicted orbit of the spacecraft Ulysses, which should allow the first observation of the northern hemisphere right–hand polarized beam of nKOM. (Note that because the time of arrival and thus the CML of Ulysses is as yet unknown, this trajectory has been drawn in Jovigraphic coordinates whereas the remainder of the diagram is in Jovimagnetic coordinates).

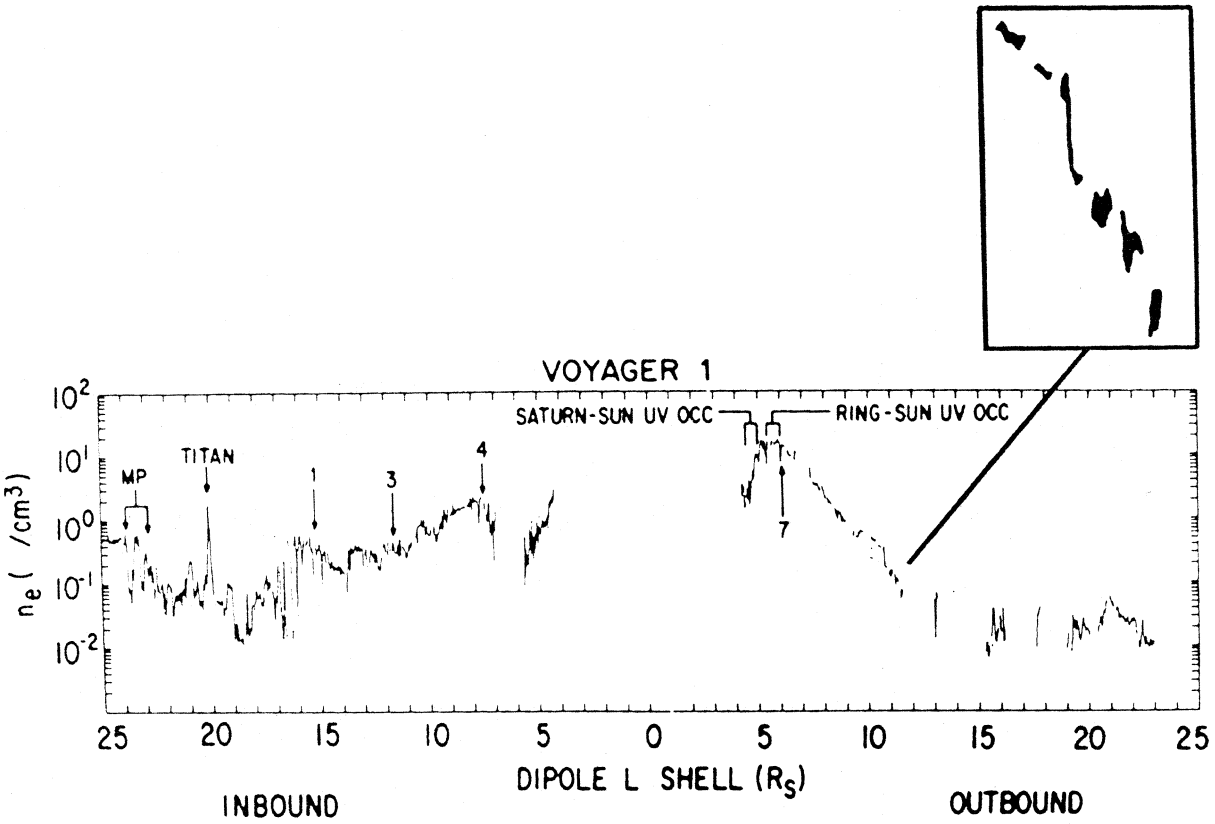

Fig. 21: Voyager 1 moment electron density, n_e, as determined before and after Saturn encounter. The inset shows the large density gradient at $L \simeq 10.6$ at which the SMR 5 kHz source is believed to be located (based on Figure 2 of Sittler et al., 1983).

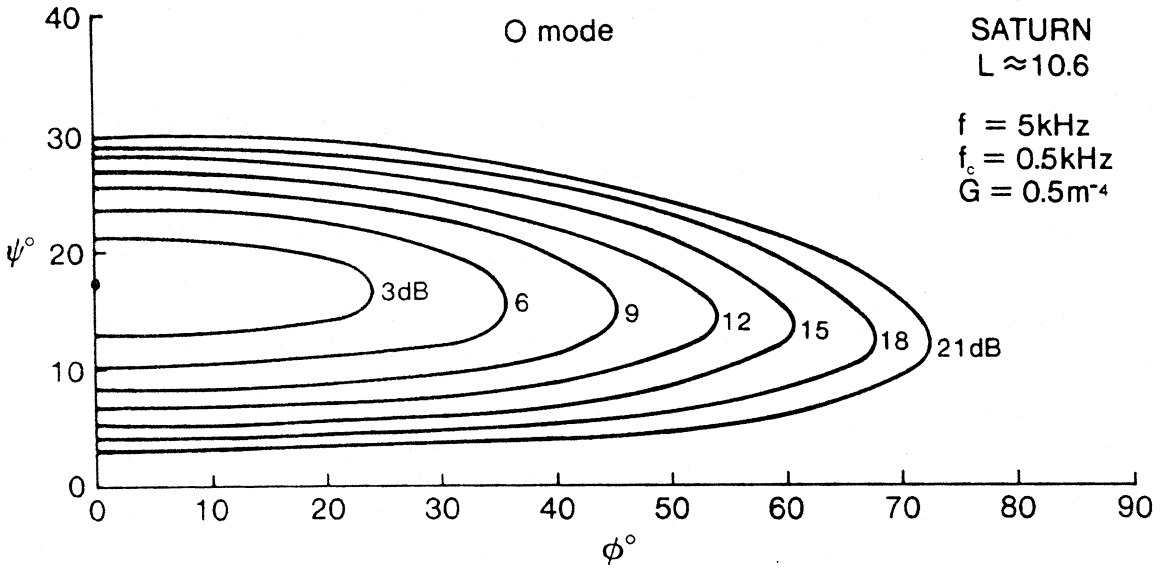

Fig. 22: The O–mode radio window computed for a source at the density gradient highlighted in Figure 21.

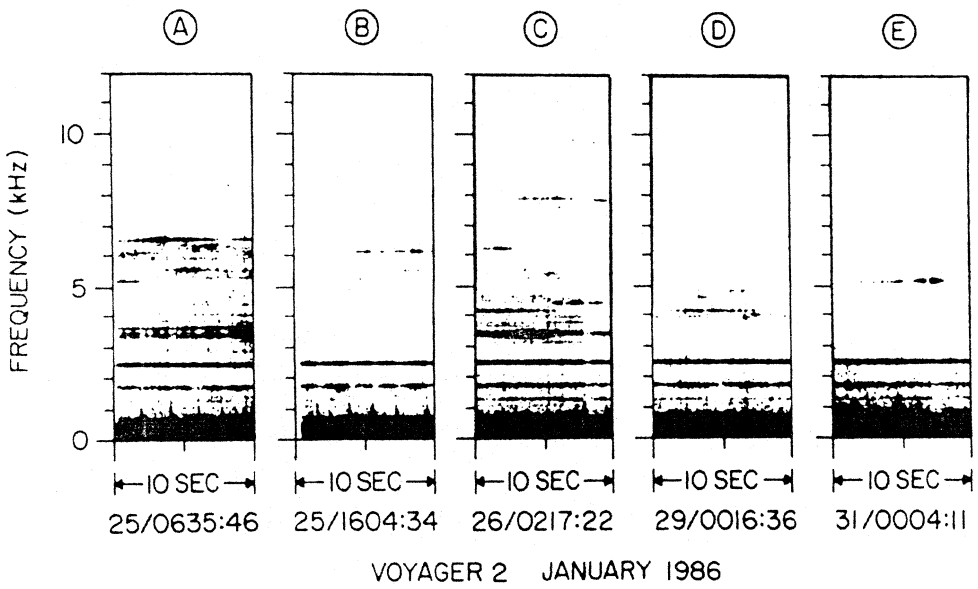

Fig. 23: A series of frequency–time spectrograms which show the detailed spectral and temporal behaviour of the bursty Uranian radio emission (from Kurth et al., 1986a). The emission is characterized by brief, narrowband bursts superimposed on a weak diffuse component. The lines at 2.4 and 1.8 kHz are spacecraft interference.

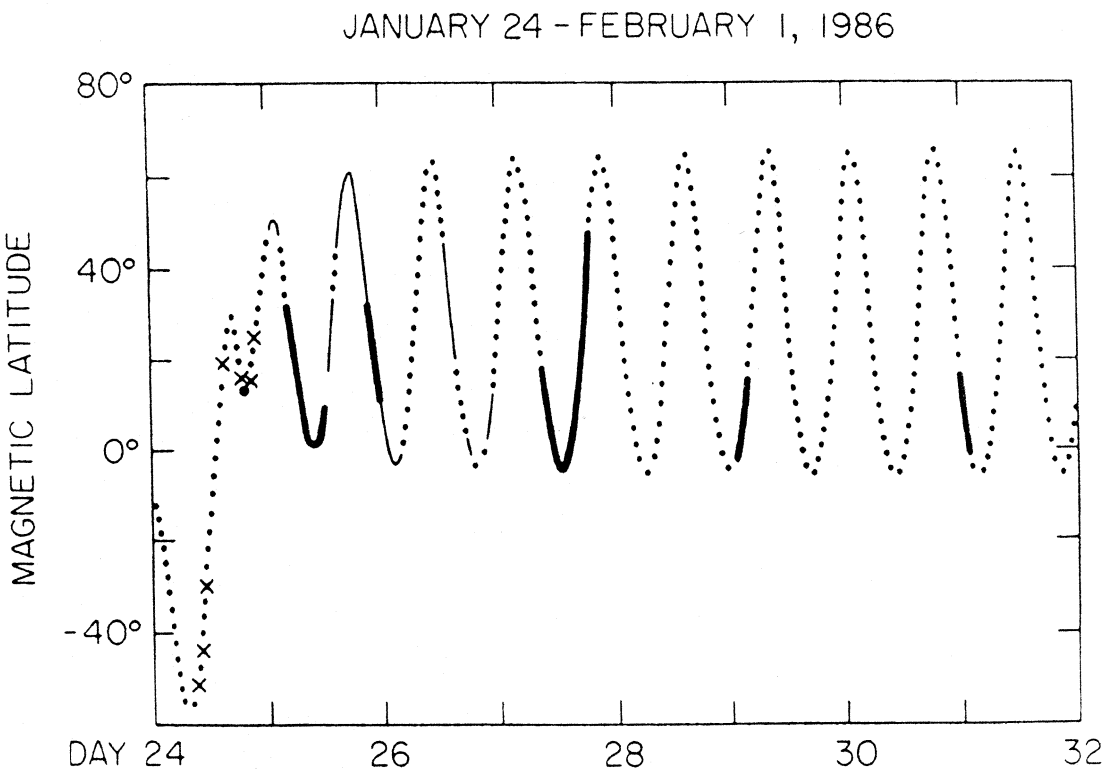

Fig. 24: A plot of the magnetic latitude of Voyager 2 as a function of time based on information on the Uranian magnetic field provided by the Voyager magnetometer. The heavy dark lines show intervals when the 5–kHz emission was prominent. The emission was only very weakly detectable in waveform samples on the inbound (dayside) leg of the encounter, indicated by "X"s (from Kurth et al., 1986a).

4. Saturn

Because of the greater distance between Earth and Saturn, the wave data from Saturn's magnetosphere do not have the same resolution in time as those from Jupiter. The nonthermal continuum at Saturn was very weak, being just above Voyager's level of detection. Kurth (1986) presented a comparison of terrestrial, Jovian and Saturnian continuum and, as little progress has been made since then, the reader is referred to that review and to Jones (1985).

As far as the author is aware, no further work has been done also on Saturnian Myriametric Radiation, SMR. Jones (1983b) proposed that SMR observed at ∼5 kHz (Gurnett et al., 1981a) was also produced according to the LMCW theory and remote–sensing indicated a source near the equator on the morning side at a distance of ∼10 R_S from Saturn. A glance at Figure 21 (from Sittler et al., 1983) shows the existence of a steep density gradient at $L \simeq 10.6$ where $f_p \simeq 5$ kHz which Jones (1983b) considered the most likely source of the 5 kHz SMR. With the relevant parameters at this location the O–mode radio window computations yield Figure 22, from which the relatively large window dimensions are apparent.

5. Uranus

Among the several types of radio emissions, discovered during the Voyager 2 flyby of Uranus (Warwick et al., 1986; Gurnett et al., 1986), were nonthermal continuum radiation at frequencies down to about 1 kHz and banded emissions near 5 kHz (Gurnett et al., 1986; Kurth et al., 1986a). The banded emission, which is observed on the nightside, has a spectrum similar to that of TMR, SMR and Jovian narrowband emissions (Gurnett et al., 1981a; 1983b) but is much more bursty and sporadic in nature, with amplitude variations of the order of 30 dB per second. Figure 23 shows a series of spectrograms (from Kurth et al., 1986a) which illustrate detailed spectral and temporal behaviour of the bursty radio emission. (The lines at 1.8 kHz and 2.4 kHz are spacecraft interference). Figure 24 (based on Kurth et al., 1986a) shows a plot of the magnetic latitude of V2 as a function of time, in which the heavy dark lines show intervals when the ∼5 kHz emission was prominent.

Kurth et al. (1986a) suggest a number of possible generation mechanisms for the bursty emissions, including wave–wave interactions (Melrose, 1981), soliton collapse (Goldman, 1983), lasing (Calvert, 1982) and the LMCW theory of Jones (1980). The latter is considered viable by Kurth et al. (1986a) because the angular motion of beams, which could produce the bursty character, seems to be assured by the dramatic tumbling motion of the magnetic field of Uranus

which is due to the 60° tilt with respect to the rotational axis of the planet (Ness et al., 1986). They suggest that it could be the large dipole tilt that is responsible for the difference between the smoothly–varying emissions from Jupiter, Saturn and Earth compared to the bursty nature of the Uranian emission. If the Uranian emission is produced according to the LMCW theory, it may be possible to derive information on the source location

by using the remote–sensing technique which was successfully applied to the emissions at the other planets. A preliminary attempt to do this by the author indicates that a possible source could lie near the magnetic equatorial plane at $9 - 10\ R_U$ where $f_c \leq 800$ Hz, which would place the source upper–hybrid frequency f_{uh} in the 6th gyroharmonic band. It may be possible then for variations in plasma density and therefore f_{uh} at the source to vary such that f_{uh} crosses gyroharmonics resulting in cyclotron damping; as for bKOM, this would result in the bursty character of the emission, which would be in addition to any beam swinging effect. An alternative explanation for the sporadic appearance of the radiation is interference between beams at the same frequency. This could arise, in the LMCW theory, from a relatively wide source from which the north and south beams overlap in certain regions. Clearly, much additional work is required to identify the Uranian emissions and their sources.

Acknowledgements: This review has benefitted greatly from discussions with the following to whom the author wishes to express his gratitude for information received: F.Bagenal, K.G.Budden, W.Calvert, J.E.P.Connerney, M.D.Desch, A.J.Dessler, D.A.Gurnett, R.B.Horne, R.L.Huff, M.L.Kaiser, C.F.Kennel, W.S.Kurth, Y.Leblanc, H.O.Rucker, E.C.Sittler, R.M.Thorne and V.M.Vasyliunas. In addition thanks are also due to R.M.Laws, D.J.Drewry and M.J.Rycroft for their encouragement over the years.